GEOSPATIAL TECHNIQUES OF DETECTING AND MAPPING LEAD POLLUTION IN SOIL USING LANDSAT 8 OLI IMAGES

BY

ALAMBA, Dauda
MTech/SET/2018/9179

DEPARTMENT OF SURVEY AND GEOINFORMATICS
FEDERAL UNIVERSITY OF TECHNOLOGY, MINNA,

JUNE, 2023

GEOSPATIAL TECHNIQUES OF DETECTING AND MAPPING LEAD POLLUTION IN SOIL USING LANDSAT 8 OLI IMAGES

BY

ALAMBA, Dauda
MTech/SET/2018/9179

**A THESIS SUBMITTED TO THE POSTGRADUATE SCHOOL,
FEDERAL UNIVERSITY OF TECHNOLOGY, MINNA, NIGERIA
IN PARTIAL FULFILLMENT OF THE REQUIREMENTS FOR THE
AWARD OF THE DEGREE OF MASTER OF TECHNOLOGY (M. TECH) IN
SURVEYING AND GEOINFORMATICS.**

JUNE, 2023

ABSTRACT

The adverse effect of high concentration of heavy metals, especially lead (Pb), in topsoil which include food scarcity, increase morbidity rate (due to lead poisoning) especially in children in the rural areas is alarming and requires an urgent attention. This research is tailored to detect and map lead polluted soil using remote sensing technique. Efforts has been made by many researchers to detect lead metals in soil especially in regions where anthropogenic activities aggravate the natural occurrence of lead (Pb). Laboratory approach which involves biological and chemical analysis is limited; quite expensive, time consuming and cannot measure extent of spread of this metal in a large area. Advances in geospatial science has brought a huge change in environmental studies. Herein, spectral analysis of lead tailings in topsoil was carried out, using Minna metropolis as a case study. Different geospatial approaches of processing satellite imageries were employed Band Ratioing, Normalized Differential Lead Index (NDLI) developed by the author and Principal Component Analysis to identify the extent of lead pollution within this study area. Results from these techniques characterized lead tailings in the study area and comparison of the performance of all techniques reveal that there is high level of consistency in their outputs, these results agree with the result of atomic absorption spectrometer test (AAS), which is the standard or conventional test. Eight (8) lead hotspots with NDLI values ranging from 13-15 were detected in the central region of the study area where built-up area is thickest, implying that human activities truly induce concentration of lead metal in topsoil. Atomic Absorption Spectrometer test carried out on soil samples taken from the identified hotspots confirm that the lead concentration in the identified areas is higher than that of other areas. The AAS results confirmed the reliability of the developed NDLI which gives higher lead index for areas with high lead concentrates and vice versa. Therefore useful information on lead polluted soil is made available to appropriate quarters for policy and decision making.

TABLE OF CONTENTS

Content	Page

CHAPTER THREE

CHAPTER FIVE

LIST OF TABLES

LIST OF FIGURES

LIST OF ABBREVIATIONS

AAS – Atomic Absorption Spectrometer

BR – Band Rationing

DEM – Digital Elevation Model

ENVI – Environment for Visualizing Images

ESRI – Environment Systems Research Institute

ETM+ – Enhanced Thematic Mapper Plus

GCPs – Ground Control Points

GIS – Geographical Information System

GPS – Global Positioning System

ha – Hectares

km2 – Square Kilometres

m - Metres

mm – Millimetres

 NDLI – Normalized Differential Lead Index

NIR – Near Infrared

OLI – Operational Land Imager

Pb – Lead

PCA – Principal Component Analysis

RGB – Red, Green and Blue

SWIR – Shortwave Infrared TIRS – Thermal Infrared Sensor

TIN – Triangulated Irregular Network

UTM – Universal Transverse Mercator

VIS – Visible

CHAPTER ONE

1.0   **INTRODUCTION**

1.1   **Background to the Study**

Lead is classified as a chalcophile under the Goldschmidt classification, meaning it is generally found combined with sulphur (Acton, 2013). It rarely occurs in its native, metallic form (Alsfasser 2007). Many lead minerals are relatively light and, over the course of the Earth's history, have remained in the crust instead of sinking deeper into the Earth's interior. This accounts for lead's relatively high crustal abundance of 14 ppm; it is the 38th most abundant element in the crust (Baird & Cann 2012). Lead is a fairly common element in the Earth's crust for its high atomic number (82). Most elements of atomic number greater than 40 are less abundant. World lead resources exceed two billion tons. Significant deposits are located in Australia, China, Ireland, Mexico, Peru, Portugal, Russia, and the United States. Global reserves resources that are economically feasible to extract—totaled 88 million tons in 2016, of which Australia had 35 million, China 17 million, and Russia 6.4 million (Bharara & Atwood 2006) As of 2014, production of lead is increasing worldwide due to its use in lead–acid batteries (Nriagu & Kim 2000). There are two major categories of production: primary from mined ores, and secondary from scrap. Lead metal has several useful mechanical properties, including high density, low melting point, ductility, and relative inertness. Many metals are superior to lead in some of these aspects but are generally less common and more difficult to extract from parent ores. Lead's toxicity has led to its phasing out for some uses (Sinha *et al* 1993).

Lead has been used for bullets since their invention in the middle Ages. It is inexpensive; its low melting point means small arms ammunition and shotgun pellets can be cast with

minimal technical equipment; and it is denser than other common metals, which allows for better retention of velocity. It remains the main material for bullets, alloyed with other metals as hardeners (Ede & Cormack 2016). Concerns have been raised that lead bullets used for hunting can damage the environment.

Lead has many uses in the construction industry; lead sheets are used as architectural metals in roofing material, cladding, flashing, gutters and gutter joints, and on roof parapets(Sinha *et al* 1993). Lead is still used in statues and sculptures including for armatures (Ede & Cormack 2016). In the past it was often used to balance the wheels of cars; for environmental reasons this use is being phased out in favor of other materials (Ede and Cormack 2016). Lead is a highly poisonous metal (whether inhaled or swallowed), affecting almost every organ and system in the human body (Nriagu & Kim 2000). At airborne levels of 100 mg/m^3, it is immediately dangerous to life and health (Harbison et al 2015). Most ingested lead is absorbed into the bloodstream (Freeman 2012). The primary cause of its toxicity is its predilection for interfering with the proper functioning of enzymes. It does so by binding to the sulfhydryl groups found on many enzymes (Freeman 2012).

The extraction, production, use, and disposal of lead and its products have caused significant contamination of the Earth's soils and waters. Atmospheric emissions of lead were at their peak during the Industrial Revolution, and the leaded gasoline period in the second half of the twentieth century (Ede & Cormack 2016). Lead releases originate from natural sources (i.e., concentration of the naturally occurring lead), industrial production, incineration and recycling, and mobilization of previously buried lead (Freeman 2012). In particular, as lead has been phased out from other uses, in the Global South, lead recycling persist in soils and sediments in post-industrial and urban areas; industrial

emissions, including those arising from coal burning Kosnett (2006) continue in many parts of the world, particularly in the developing countries (Langmuir & Broecker 2012).

Lead can accumulate in soils, especially those with a high organic content, where it remains for hundreds to thousands of years. Environmental lead can compete with other metals found in and on plants surfaces potentially inhibiting photosynthesis and at high enough concentrations, negatively affecting plant growth and survival. Contamination of soils and plants can allow lead to ascend the food chain affecting microorganisms and animals (Langmuir & Broecker 2012).

In general, heavy metals pollution is still one of the major and continuous environmental hazards been faced globally (Yuan *et al.,* 2018). Heavy metals are elements occurring naturally and are characterized by their high atomic weight and are five times denser than water (Fergusson, 1990). Ming-Ho (2005) also regarded metallic elements which have an atomic weight higher than 40.04 (the atomic mass of calcium) as heavy metals. These metals are widely relevant and applicable in technology, industrial, agricultural, domestic and medical fields; this consequentially induce their wide distribution and spread in the environment. Heavy metals escape into human surroundings through man-made and natural sources. Expanding these duet sources, industrial, agricultural, geogenic, pharmaceuticals, atmospheric sources and domestic effluents are the reported sources of heavy metals (He *et al.,* 2005).

Heavy metals have been categorized according to their relevance, requirements in humans and other ecosystems, physiological and biochemical functions, their prevalence, those having trace concentrations known as trace elements among others. Cobalt (Co), chromium (Cr), copper (Cu), iron (Fe), nickel (Ni), selenium (Se), zinc (Zn), magnesium (Mg), manganese (Mn), and molybdenum (Mo) are example of heavy metals

categorically required for several organic functions (WHO, 1996). Unfortunately, as some of the naturally existing metals are of noble and precious significance (such as gold), some including arsenic (As), antinomy (Sb), aluminum, platinum (Pt), lead (Pb), beryllium (Be), bismuth (Bi), cadmium (Cd), gallium (Ga), Germanium (Ge), indium (In), gold (Au), tellurium (Te), are considered as non-important metals and also have no established biological functions (Chang *et al.,* 1996).

Lead is a bluish-grey metallic element which non-mechanically exists in the Earth's crust in a minute amount. Although it ensues naturally in the surrounding, man-induced undertakings such as mining, burning of fossil fuels and productions add to its discharge in concentrations that are high (Oehlenschlager, 2002). It is one of the most noxious metals occurring naturally on Earth and yet the fifth most exploited metal in advanced countries like U.S (Abdullahi, 2013). The metal becomes toxic to human when they compound in the soft tissues due to inability of the human system to process them. Intake of this metal becomes almost unavoidable, it enters into the human body via water, air, food or preoccupation through skin in industry, pharmaceutical, agriculture, residential or manufacturing setups.

Nigeria is one of the developing countries faced with health complications and disruption in ecosystem due to lead poisoning. Lead harming in soil was found out first in Zamfara state of Nigeria by Medecins San Frontieres (Doctors without Borders, 2010). The plague, sourced from gold exploration from refining lead-rich rock ores, hence, leading to pollution caused the death of over 400 kids in the province. To initiate the beginning of treatment, 8 villages were remediated. In 2015, about 5 years after the lead poisoning outbreak in Zamfara, there was a reoccurrence of the situation in Niger State. This also came about due to hazardous mining operations. Unfortunately, over 2500 members of

the community were made to experience the plaque out of which 30 kids died. Within the state, two villages were remediated and for more than a year, treatment was undertaken (Ifeoluwa, 2018). These occurrences within the country are indications that the environments of industrial activities such as mining, agriculture, and others are likely to be polluted by this heavy metal. In other words, the spatial distribution of lead in the environment becomes a mystical concept. In support of this, notwithstanding the acknowledgment that the metal (Pb) is an ecological and civic hazard affecting health of universal magnitudes, yet the geographical coverage of Pb poisoning in the developing countries is still poorly known. This is traceable to the continuing absence of data for detecting and recognizing regions polluted by lead which consequentially affects the ecosystem through poisoning. Nevertheless, putting the supreme purpose of soil into consideration, especially for securing the world's need for food, human health, growing size of urbanization, it is imperative to recognize and control lead contaminated sites (Henke & Petropoulos, 2013).

Several methods for lead detection and analysis have been developed over the decades. Fu and Wang (2011) expounded that techniques of detecting lead pollution in soil include traditional, thermal, physical, and further approaches involving chemical processing. However, these methods, many times show severe limitations including expensiveness, disproportionate work expenditure, hostile change of soil compositions and microfloras. Several other studies have identified the conventional methods always requiring field sample collection, several laboratory analysis and other biological inputs to be slow, expensive and tedious, hence, the need to utilize a faster approach (Yuan *et al.,* 2018; Daniel *et al.,* 2019).

Geospatial techniques including Geographical Information System (GIS), Global Positioning System (GPS), Remote Sensing (RS) and so on are widely applicable in scientific studies. Out of these techniques, remote sensing has diverse applications and has been employed in various fields of science. This is due to the capability of remote sensing satellites to cover large extent of areas and to collect diverse information about the areas of coverages. Classifying the many remotely sensed data, hyperspectral images are the most utilized kind of satellite data for scientific studies. Salim *et al.* (2019) said that developments caused by technology in hyperspectral RS have been extensively taken advantage of in researches involving contamination of soil by heavy metal, in a rapid less costly manner, the technologies can proffer assessments of Pb contamination. These hyperspectral images include Landsat images (ETM 4+, 5, 7 and 8 OLI), Sentinel image (2A, 2B, 3A, 3B) and so on. This study seeks to investigate the applicability of geospatial technique for detecting and mapping lead pollution in soil using Landsat 8 OLI images.

1.2   Research Questions

i.   Are there traces of lead in the study area?

ii.   How can these traces of lead presence in the study area be located?

iii. Is the concept of adopting geospatial technique reliable in detecting and mapping lead presence in the study area?

1.3   Problem Statement

The rapid growth of human settlements and urbanization has resulted into serious problems of environmental pollution which included large quantities of waste gas, wastewater, and solid waste that discharged into the environment. The contaminants in the soil at a certain level brings about deterioration or loss in some of the natural soil properties. Lead is a very common soil contaminant associated with developing countries like Nigeria. Therefore, it is a health related problem which affects all living things in the

Environment. Lead poisoning is a health related situation and brings about an evolving concern on the environment at large. Globally known approaches for inspecting soil pollution premised on sampling soil locations and analysis involving use of chemicals takes a lot of time, expensive and occasionally integrate the use of chemicals that cause ecological (environmental) damages. Therefore, there is a need to develop a low-cost geospatial method for detecting the spatio-temporal pattern of lead pollution in the soil at areas where activities that could trigger pollution take place

1.4 Justification

A dependable and ecologically friendly technique is required to speedily find out lead soil pollutants at any phase for the analysis and definition of supposed polluted locations, also for monitoring rehabilitation progressions... Remarkably, every Earth objects (man-made and natural) reflects and emits electromagnetic radiation through an array of wavelengths in its own distinguishing manner, according to its physical state and chemical composition (Avery & Berlin, 1992). This inherit characteristics of the soil makes it possible to capture and record information about Earth object or layout on hyperspectral images in Remote Sensing. On the other hand, Niger State has also been plagued with lead poisoning due to pollution of the environment with lead metals, resulting from industrial activities such as mining. Ifeoluwa (2018) stated that about thirty (30) children died of lead poisoning in 2015 and over 2500 communities were infected. In fact, treatments are still ongoing on affected persons in the state. Hence, the need to map and monitor lead pollution in the state. Hence, for proper mitigation and assessment, this study seeks to employ geospatial technique for detecting and mapping of lead pollution in soil within Niger State, using Landsat 8 OLI images.

1.5   Aim and objectives

The aim of the study is to use Landsat 8 OLI to detect and map lead (Pb) pollution in soil by the application of geospatial techniques, below is the objectives

i.   To conduct experimental analysis for identifying unique spectral signature that corresponds to heavy Pb pollution in top soil using Landsat 8 OLI imageries.

ii.   To carry out mapping of lead presence in the study area

iii. To perform Normalized Differential Lead Index (NDLI) and validate results with Atomic Absorption Spectrometer (AAS) test.

1.6   Study Area

This study was exemplified over Minna metropolis. Minna Metropolis is the most populated part of the capital city of Niger State in Nigeria. This geographical location (as seen in figure 1) is Latitude 9°37'55''North and Longitude 6°33'24'' East. It occupies an area of about 12200 hectares of land. As presented in Figure 1, it is bounded in the North by Shiroro Local Government, in the East by Munya Local Government, to the West by Bosso Local Government and to the South by Paikoro Local Government areas. The population of the city is estimated at 304,113 (National Population Census 2006) and there are a lot of industrial activities carried out within the area.
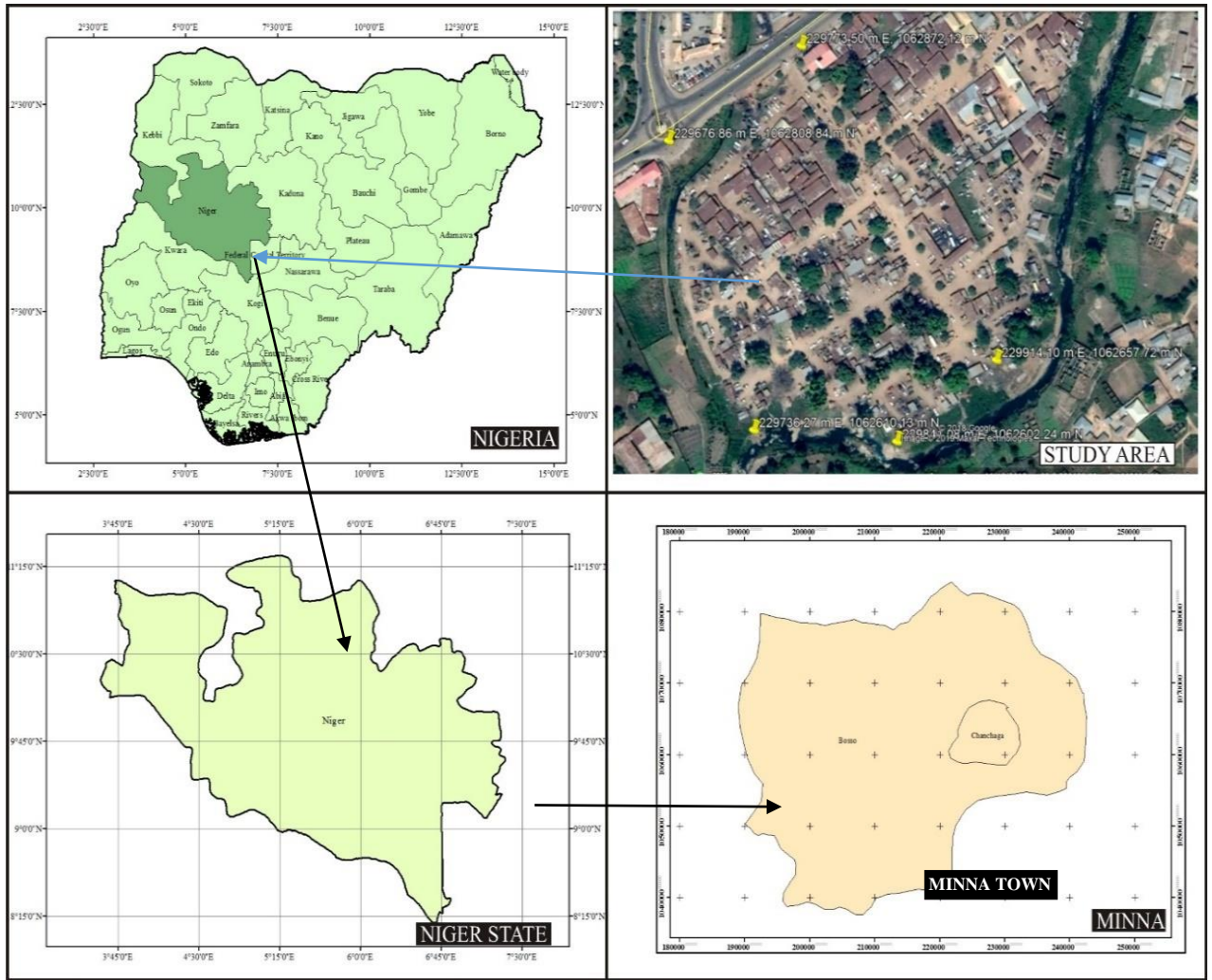
Figure 1.1: Study area

Source: Niger State Ministry of Land and Survey

CHAPTER TWO

2.0   LITERATURE REVIEW

2.1   Heavy Metals

In the Earth's crust, metals just exist without any processes and their composition differ in locations, bringing about geographical dissimilarities of surrounding concentrations (Khilifi & Hamza-Chaffai, 2010). Heavy metals are regarded as those metals which have a specific density of more than $5 gcm^{-3}$ and harmfully affect the environment and living organisms (Jarup, 2003,). Among the thirty-five naturally existing metals, twenty-three possess high specific density with atomic weight greater than 40.04 are those regarded as heavy metals and include: antimony, bismuth, cerium, cadmium, cobalt, arsenic, gallium, tellurium, chromium, copper, gold, lead, iron, mercury, uranium, manganese, vanadium, zinc, platinum and silver.

Metalloids generally incline to produce bonds that are covalent, which causes them to display properties that are toxicological in nature. Covalently binding with organic groups is the major significance of such property, hence, forming lipophilic ions and compounds; when they bind to nonmetallic components of biological macromolecules, they can have harmful consequences (Jessica *et al.,* 2020). Metals cannot be split and are non-biodegradable. By encapsulating the active component in a protein or storing them in intracellular granules in an insoluble form to be expelled in the organism's feces or for long-term storage, organisms can detoxify metal ions. When inhale or swallow heavy metals, they bio-accumulate in body systems, hence classified as dangerous.

Many of these heavy metals already exist naturally in the ecosystems around us and are harmless in a very low concentration, in fact, at this concentration, they are very essential to maintain various physiological and biochemical functions in living organisms (Adriano, 2001 and Abdullahi, 2013). Figure 2.1 shows a diagrammatic representation of

springs of heavy metals in the surroundings. Natural deterioration of the earth's crust, mining, soil erosion, industrial discharge, urban runoff, sewage effluents, pesticides or medications used to treat diseases applied to plants, and air pollution fallout are a few examples of these sources, coal burning in power plants, petroleum combustion, wood preservation and paper processing plants, nuclear power stations and a number of others (Ming-Ho, 2005). Environmental contamination can occur through metal corrosion, soil erosion of metal ions, leaching of heavy metals and atmospheric deposition, smelting operations, industrial production and use, sediment re-suspension, metal evaporation from water resources to soil and ground water (Nriagu, 1989; He *et al.,* 2005, Beyersmann and Hartwig 2008). Natural activities such as volcanic eruptions and weathering have been additionally reported to noticeably add to heavy metal pollution in the environment. Additionally, heavy metal contamination has been caused through the usage of heavy metals in agriculture, such as the use of fertilizers, insecticides, pesticides and others (Jessica *et al.,* 2020). Although some people are mostly exposed to these toxins at work, for the majority of people, exposure to these harmful substances comes mostly from their diet food and water (Lenntech, 2018; Duffus 2002). Heavy metal contamination nearly always occurs in a cyclical order: industry, atmosphere, soil, water, foods, and people. The economic importance of these metals have made them practically unavoidable in our environments; among these metals exist precious and noble elements including indium, gold, silver, rhodium and platinum (Rao & Reddi, 2000). Many of them are of outstanding industrial importance such as tin, lead, copper, tungsten, zinc iron and so on, of recent, they serve as the core atom of synthetic bioinorganic catalysts that are used for particular chemical processes (Terfassa *et al.,* 2014).

In contrary, many of these metals readily exert toxic effects even at low concentration. Example of such we have mercury, arsenic, lead, thallium, cadmium, chromium, etc
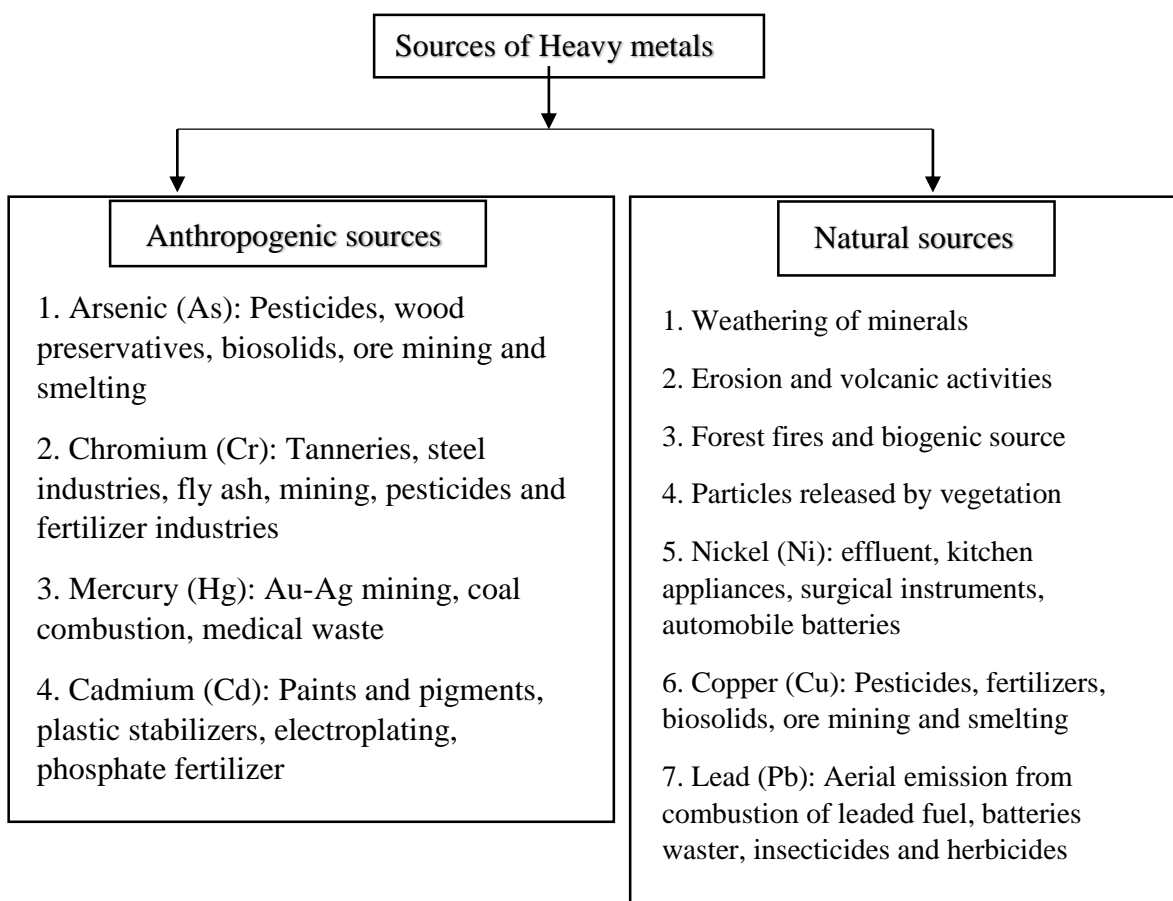
Figure 2.1: Sources of heavy metals in the environment (Source: Ravindra and Narendra, 2018)

2.1.1   Heavy metals toxicity

Numerous health hazards are connected to heavy metal toxicity, which has emerged as a serious threat. For ecological, evolutionary, nutritional, and environmental reasons, heavy metals are significant environmental contaminants, and their toxicity is a problem that is becoming more and more important (Freeman, 2012). Though they do not have any biological role, the toxic effects of these metals continuously exist in the form hazardous to the human body and its normal operation they become poisonous when they surpass some concentrations threshold (Monisha *et al.,* 2014).

Toxicity of heavy metals increase is an effect of localization of a high quantity of the metals. Though essential metals are vital in the body, both the excess and insufficiency can harm human's system. The toxicity mechanism of heavy metals in human body include alterations in the permeability of the cell membrane, suppression of protein synthesis, variations in nucleic acid function, and inhibition of enzyme activity (Bernado, 2020). Generally, heavy metal toxicity includes neurotoxicity, hepatoxicity and nephrotoxicity (Jessica, 2020).

2.2   Soil Pollution by Heavy Metals

Major source of heavy metals in soil are:

i.   Geochemical origin;

ii.   Mining and smelting, agricultural products (fertilizers, pesticides, sewage sludge, etc.), the burning of fossil fuels, the metallurgical and chemical industries, sports, and the production of weaponry for the military are examples of human activities.

iii.   Atmospheric deposition (Alloway, 1995).

Pollution is regarded as the introduction of chemicals or energy forms which are capable of endangering human health, causing harms to ecological and living resources, damaging the structures or amenity of interference with legitimate uses of the environment by human being. Soil pollution which can be either deliberate or not is the introduction of such chemicals or energy form into soil. Deliberate soil pollution includes pesticides, fertilizers, animal manures, spills of petroleum distillates, byproducts of coal combustion, and garbage disposal, among others. Non-deliberate pollution of soil by heavy metals may include flooding of seas and rivers which accumulate contaminated water and sewages to the land and accidents of vehicles transporting harmful chemicals. Since weighed metals are non-biodegradable, they last a very long time in the soil because they

cannot degrade through microbial or chemical processes. (Aronsson & Perttu, 2001; Walker *et al.,* 2012). These heavy Metals in the soil pose dangers to the entire biosphere and are ingested directly. (leaving the children to the highest risk), absorbed by plants, changing the soil's characteristics and posing risks to both the plant and the plant's food chain, including its pH, colour, porosity and natural chemistry, hence, impacting the quality of the soil (Muchuweti *et al.,* 2016; Gupta *et al.,* 2012).

Among these massive metals, five are known to have negative health consequences on numerous organ sites, even at low exposure levels. These are lead, arsenic, mercury, cadmium and cadmium (Tchonwou, 2012); they all have a long history of usage and have gotten into our environment, causing unwelcome collateral exposure. This study focuses on soil pollution due to lead contamination.

2.3   Lead (Pb)

Lead is one of the most abundant massive metals (Seema *et al.,* 2013) and is the most significant heavy hazardous substance in the environment. As a result of its paramount physico-chemical attributes, its use dates back to ancient times. Ironically, explained that its important properties such as malleability, softness, ductility, poor conductibility and its resistance to decomposition make it difficult for humanity to avoid its use. It is established that due to its non-biodegradable nature and continuous use, its concentration accumulates in the environment, hence increasing its hazardous effects on the environment.

Lead though occurs on the Earth's crust naturally due to the formation of the Earth. However, due to the utilization of heavy metals, there will soon be an increase in metallic materials in the aquatic and the terrestrial environments. In other words, anthropogenic activities including fossil fuels burning, manufacturing and mining add largely to the discharge of lead in high concentration. This is expected since it has wide applications in

different domestic, industrial and agricultural operations. Currently, this heavy metal is used in the production of lead-acid batteries, metal products (such as pipes and solder), and x-rays shielding gadgets (Gautam *et al.,* 2016).

2.3.1 Sources of lead pollution in our environment

According to Langmuir & Broecker (2012), environment is the surroundings within which humans exist. These include water, land and the atmosphere of the Earth; micro-organisms, animal and plant life, interactions between them, as well as the physical, pharmacological, aesthetic, and cultural aspects of such that have an impact on human health and wellbeing. There are various aspects of the environment that affect how it behaves and its inherent worth. The most significant of which is the biosphere since it houses the living organisms. It is in it that organisms living are found (animals and plants) interrelating with their inorganic environment (soil, water and air). Lead in our environment can come from anthropogenic and natural processes and end up in many environmental compartments (soil, air, water and their interface). The following sub-section explains the natural and anthropogenic processes that bring about lead in our environment

2.3.1.1 Natural sources

A lot of studies has documented different natural sources of lead as one of the heavy metals. Such natural emissions that bring about the release of lead into the environment includes sea salt sprays, volcanic eruptions, forest fires, rock weathering, biogenic sources and wind-borne soil particles. Lead may be released naturally from the endemic spheres of rocks into various environmental compartments. This heavy metal can be seen in hydroxides, sulphides, sukphates, phosphates, silicates and organic compounds form (Herawati *et al.,* 2000).

2.3.1.2 Anthropogenic sources

By anthropogenic, we refer to man-induced activities that results into the emission and release of lead into the environment. Pollutants are released into various environmental compartments as a result of agriculture, industries, wastewater treatment, mining, and metallurgical operations. Lead-related anthropogenic processes are thought to go beyond natural fluxes. The majority of the naturally occurring metals in wind-blown dusts come from industrial locations. Remarkably, some significant anthropogenic activities that result in the release of lead metal (and as a pollutant) into the environment includes automobile exhaust and blacksmithing. However, these largely contribute to the increasing environmental pollution as a result of daily manufacturing in order to meet the demand of large populations.

2.3.2 Lead poisoning

When absorbed by the body, the potentially harmful element lead (Pb) builds up in the blood and bones as well as in organs like the liver, kidneys, brain, and skin (Angelika & Jeffrey, 2020). Lead has been demonstrated to interfere with the hepatic, endocrine, reproductive, gastrointestinal and immune systems in human (Harbison *et al* 2015). To this effect, lead is known to have metabolic and genetic effects. Lead interferes with a number of metabolic processes, including calcium and protein reactions. Having entered into human body, taking the place of calcium, pb interacts with biological components, disrupting their normal operation. It decreases the operation of numerous enzymes, leading to alteration in their structure, and competes with essential captions for binding sites, hence reducing their action.

Established that the primary mechanism causing lead's toxicity is oxidative stress, thereby affecting the configuration of fatty acids in membranes (negatively influencing processes

such as signal transduction, endocytosis and exocytosis). This heavy metal can also lead to alterations in expression of gene. Also, the body's antioxidant reserves may be rapidly depleted by lead exposure, and reactive oxygen and nitrogen compounds may be produced at higher rates. As a result, reduced glutathione reeducate levels result from increased oxidative stress, which lowers the antioxidant's concentration. (Nriagu & Kim 2000). A summary of the properties, uses, effects (due to poisoning) and sources of lead is shown in table 2.1

Table 2.1: Lead uses, properties and effects (Source: Haynes, 2011)

Properties	Uses	Effects in Human	Sources in food
- Density: 11.3 g/cm3, - 37th most abundant metal, - Found in a mineral ore known as galena, which is made up of lead sulphide and can be combined with silver, zinc and copper. - Dull silver-grey metal - Soft - Easily worked	- Used in the past for: ∘ Hair dyes, ∘ Pottery lead glazes, ∘ Insecticides, - Lead-acid batteries in cars, - Computer screen sheets to safeguard from radiation, - Ammunition and projectiles - Lead crystal glass, - Cable sheeting, - Sports equipment, - Weight belts for divers, - Canister for corrosive liquids, - In buildings for roofing - Stained glass windows, - Lead piping	- Hypertension, - Miscarriages, - Premature and low births, - Stillbirths, - Renal impairment, - Brain injury, - Abdominal pain, - Pica, - Peripheral nerve damage, - Sperm damage, - Encephalopathic signs, - Iron deficiency due to disruption of haemoglobin synthesis, - Cognitive impairment, - In children: ∘ Brain and central nervous system development altered ∘ Reduced intelligence, ∘ A decline in educational achievement, ∘ A reduction in the attention span, ∘ Increase in anti-social behaviour	Fruit and vegetables, _ Grains, _ Seafood, _ Red meat, _ Wine, _ Soft drinks

2.3.2.1 Toxicology processes of lead

Blood pressure rises as a result of prolonged lead exposure. Lead has a negative impact on important hormonal and neurological systems and regulates cardiac output, peripheral vascular resistance, and heart rate. Nitric oxide is essential for controlling blood pressure through peripheral and central processes and is reduced in lead-induced hypertension in rats. ROS activity and reactivity with NO are both correlated with NO, which is formed from oxidative stress. Lead alters the cell-signaling processes found in endothelial cells, which results in disruption of the NO vasodilatory activities. Lead exposure reduces the expression of the soluble guanylate cyclase. This enzyme creates cyclic GMP, which facilitates NO-induced vasodilation. Lead-induced hypertension is linked to adrenergic system abnormalities, which include raised plasma norepinephrine levels, increased activity in the central sympathetic nervous system, and decreased density of vascular β-adrenergic receptors.

The stimulation of the sympathetic nervous system either directly or indirectly activates the renin-angiotensinaldosterone system. Chronic exposure to lead causes an increase in plasma renin activity, plasma aldosterone levels, and plasma angiotensin-converting enzyme (ACE). Alterations in the control of the kallikrein-kinin system and the synthesis of the vasodilator hormones are both associated with hypertension. Lead has contraction effects on vascular smooth muscles, which are brought on by the inhibition or activation of Na-K-ATPase and the elevation of Ca^{2+} levels in the cells, possibly owing to activation of the protein kinase C (Jessica *et al.,* 2020).

Lead interacts to a number of proteins in renal cells, some of which have been linked to lead toxicity. The proximal renal tubule forms intra-nuclear inclusion bodies, which results in lead nephrotoxicity. Lead complexed with protein makes up the nuclear inclusions, which are linked to a change in how lead is compartmentalized from the

cytosol to the nuclear fraction. When it comes to lead uptake into the nucleus, cytosolic proteins like 2-microglobulin cleavage products can act as carriers or other intermediary ligands. The ligand exchange reactions to additional cytosolic binding sites may also include cytosolic proteins, such as δ-amino-levulinic dehydratase, that binds and which lead impedes. In contrast to the inducers of zinc and cadmium, metallothionein can also be bound to lead but does not cause the protein to be produced. In the mitochondria found in the cells of the renal proximal tubule, which have aberrant respiratory functions and a lower respiratory control ratio, structural abnormalities are observed. Additionally, the succinate- or pyruvate/malate-facilitated respiration. Lead enters as a substrate for a calcium transporter in the isolated renal mitochondria, where it inhibits calcium uptake. Impairment of oxidative metabolism may be a factor in cellular aging and transport deficiencies. Lead exposure also results in oxidative stress, and the kidneys' secondary reactions to lead include the activation of NO synthase, transketolase, and glutathione S-transferase in the kidney. Lead lowers both the renal blood flow and the glomerular filtration rate, according to in vitro experiments in rats. Additionally, proximal tubule damage and impairment, glomerulus sclerosis, which impairs renin release and/or renal insufficiency, may also be the cause of hypertension (Ede and Cormack 2016).

Lead has also been seen to have an impact on the haematopoietic system in both humans and animals, where urine porphyrin levels as well as levels of ALA, FEP, EP, ZPP, coproporphyrin, and anemia rise.

Lead affects the haem production by interfering with the activity of the enzymes ALAS, ferrochelatase, and ALAD. Lead indirectly stimulates the mitochondrial enzyme ALAS, which then catalyzes the reaction of succinyl-coenzyme A and glycine condensation to produce ALA. Lead inhibits the cytosolic enzyme ALAD, which includes zinc, by catalyzing the condensation of two ALA molecules to generate porphobilinogen. Lead

binds to the vicinal sulphydryl in the ALAD's active site, inhibiting it noncompetitively. Due to the inhibition of ALAD and the feedback derepression of ALAS, ALA accumulates. Lead has a non-competitive effect on the mitochondrial enzyme ferrochelatase, which contains zinc. In Kabata-Pendia (2001), the reduction in operation facilitates the production of Fe^{2+} in the protoporphyrin ring, leads to the formation of heam. Lead may block ferrochelatase by attaching to the vicinyl sulphydryl group in the active site, which results in a buildup of protoporphyrin IX present in the circulating erythrocytes as ZPP. Only erythrocytes that are produced in the erythropoietic area and are exposed to lead exhibit ZPP accumulation. Blood hemoglobin levels drop as a result of the interference with hemoglobin synthesis. Hypochromic, normocytic anemia, associated with reticulocytosis, results from a decrease in the generation of hemoglobin and an increase in the destruction of erythrocytes.

Lead has a number of mechanisms that impact the neurological system, one of which is calcium action mimicking and/or disruption of calcium homeostasis. PKC, a protein kinase, is involved in a number of crucial synaptic transmission pathways.

Similar to the production of neurotransmitters, ionic channel conductance, ligand-receptor interactions, and dendritic branching are these activities. The PKC family consists of 12 isozymes, and each one's needs for the enzymatic cofactor, cellular distribution, and tissue expression are unique. The γ -isoform of PKC, one of the calcium-dependent forms of the enzyme, may be a target for lead neurotoxicity. One form of PKC that is calcium dependent and may be a target for lead neurotoxicity is the γ -isoform. Through the AP-1 promoter elements, the AP-1 transcriptional regulatory complex, which is formed by PKC, regulates the expression of a large number of target genes. Glial fibrillary acidic protein (GFAP), an astrocytic intermediate filament protein, is regulated by lead through the AP – 1 promoter and is induced when there is reactive astrocytic

gliosis. Endothelial cells and astrocytes make up the blood-brain barrier. Yusuf *et al.,* (2015) Lead has been proven to prematurely activate PKC, which affects the development and operation of the brain's microvascular system. Gross blood-brain barrier abnormalities were observed at high lead exposure levels, which can result in an acute lead encephalopathy where chemicals, ions, and water can freely enter the brain. Because the lymphatic system in the brain is underdeveloped, the clearance of the plasma contents happens slowly, oedema develops, and the intracranial pressure increases as a result. Lead toxicity will be more likely since the blood-brain barrier of the foetus is still developing. Another enzyme that is affected by lead metal is Calmodulin. Eukaryotes have calmodulin, which is a crucial intracellular calcium receptor. Calcium causes a conformational shift in calmodulin that converts the protein into an active state. The enzyme is not adequately activated in the presence of lead (Aloysius et al 2013).

Lead has been proven to prevent the induced release of acetylcholine, which results in decreased cholinergic function, as seen in the peripheral and central synapses. Lead decreases the release of acetylcholine by blocking calcium entrance into the neuromuscular junction terminal. Lead, however, also hinders the organelles' ability to reassume their possession of intracellular calcium, leading to an increase in the neurotransmitter's spontaneous release. Lead can block the nicotinic cholinergic receptors, according to in vitro research. It is unknown whether this activity also takes place in living organisms or whether lead affects how nicotinic cholinergic receptors are expressed in a growing brain. Most evidence points to the visual cortex as the only area where the metal directly affects muscarinic receptors. Lead has been found to directly inhibit muscarinic receptors that are found in the rods and bipolar cells of the retina in the visual cortex (Simba et al 2018).

2.3.2.2 Lead poisoning in children

Studies have shown that the category of human being that suffer mostly from lead poisoning is the children. World Health Organization (WHO) recently continue to emphasize the essence of managing lead amongst children, because researches constantly reveal that such exposures affect their central nervous system and development (WHO, 2016). This heavy metal especially harmfully affects children below 6 years old, most likely due to the rapid development and growth of the brain, which is accompanied by periods of increased vulnerability, and the high demand for nutrients (WHO, 2016). Children who encounter severe lead poisoning may experience hearing loss, behavioral issues, hyperactivity, agitation, headaches, muscle twitches, hallucinations, learning or behavioral challenges, hyperactivity, or agitation. On the other hand, acute lead poisoning in youngsters can cause paralysis, coma, and convulsions. In disastrous situation, edema and alterations in the blood vessels might cause catastrophic brain injury. (Tamayo *et al.,* 2016).

A summary of the symptoms and associated diseases due to lead exposure in children is shown in figure 2.2
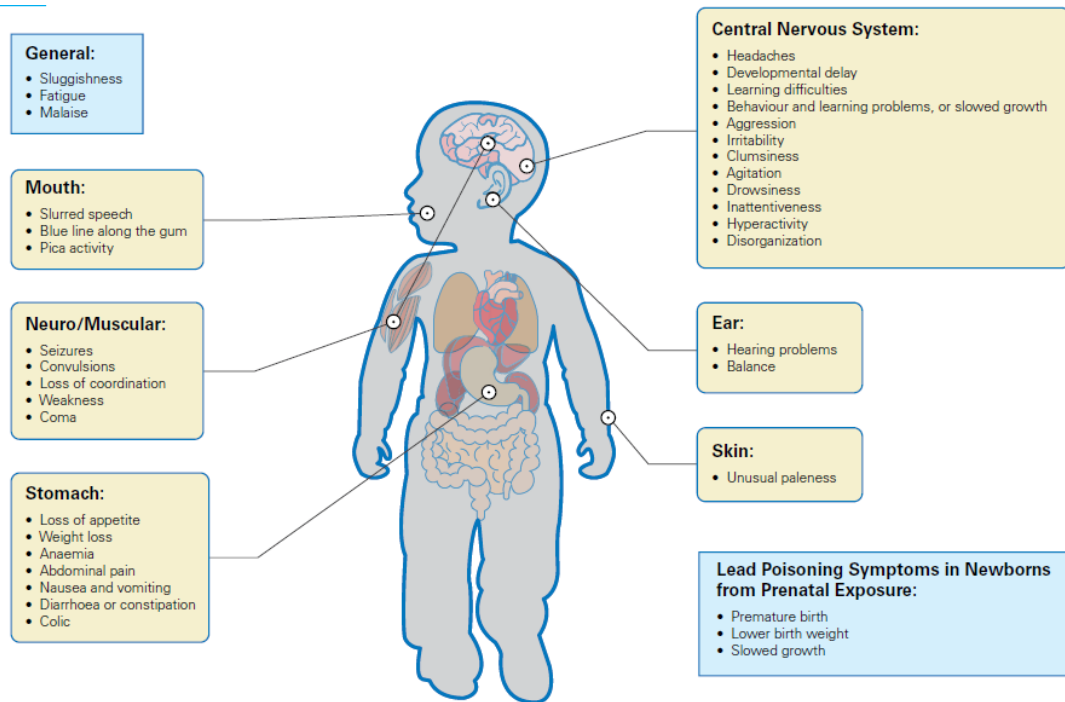
Figure 2.2: Lead poisoning symptoms in children (Source: WHO, 2019)

Children are widely exposed to environmental lead through ingestion and inhalation. Compared to adults, inhalation adds to higher levels of blood in children. The main sources of Pb in children are dirt, dust, and food, while drinking water is typically a less significant source. (Figure 2.3). The typical infant and toddler behaviors of sampling objects, placing hands in mouths just after playing, etc. greatly increase the exposure of young children to lead. (Tamayo *et al.,* 2016). Young children who reside in Pb-contaminated surroundings are more likely to consume potentially harmful substances. In families where one parent works in a lead-contaminated area, the risk of lead poisoning is increased. Pb-exposed parents frequently transfer lead dust from the office into the home on their skin or clothing, increasing the likelihood that their kids will be exposed to workplace lead.
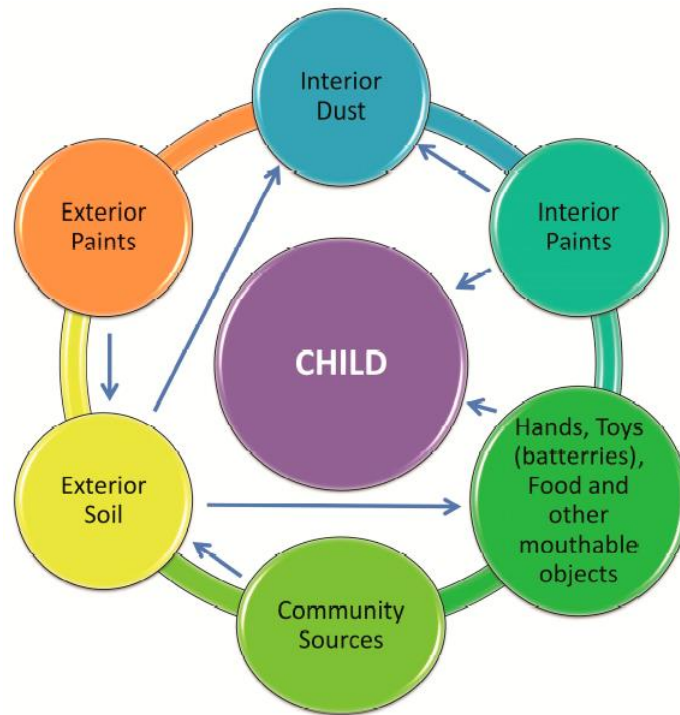
Figure 2.3: Domestic likely sources of lead poisoning among children

As shown in figure 2.3, it is obvious that the largest source of lead exposure and poisoning in children is from lead-contaminated soil. Therefore, to mitigate the increasing effect of lead poisoning in children, early detection and spread of lead in contaminated soil is required. Several studies however, have recommended that monitoring of Pb content in children's blood should be done, since they are most vulnerable (atsdr.cdc.gov; ATSDR, 2017; ATSDR, 2019; Tamayo *et al.,* 2016)

2.4 Related Works on Detection of lead using Geospatial Techniques

The increase in industrial activities in recent times has resulted into a corresponding rise in the discharge of heavy metals on soil surfaces causing serious environmental pollution (Tamayo *et al.,* 2016). The assessment and mapping of soil heavy metals can assist the development of strategies to promote sustainable use of soil resources, decrease soil degradation and expand crop production. Remediation of soils polluted by heavy metals is a major global ecological issue. Remote sensing is one of the most important methods used for soil survey, mapping and environmental investigations (Lillesand and Kiefer

2003). Geostatistical interpolation is used to survey and interpret the spatial distribution of pollutants in soil (He and Jia 2004; Woo et al., 2009). The inverse distance weighted (IDW) function is helpful when the purpose is to investigate overall pollution patterns (Zheng 2006). The Middle Nile Delta is affected by different pollution sources, because of the increasing number and types of industries, urban expansion, increased traffic volumes, use of drain-water and waste deposits (Abu Khatita 2011). The latter may well present a long-term danger. Usually waste deposits just settle within the normal Nile sediments and no special effort is made to construct barriers, which hinder the migration of water from these deposits into ground-water. High concentrations of vanadium (V) can damage human health, while the inhalation of airborne V-compounds can affect eyes, throat and lungs, produce weakness, ringing in the ears, nausea, vomiting, headaches and damage nerve systems (Lagerkvist, Oskarsson 2007). In Egypt, measured chromium (Cr) contents in soils range between 11.6-179 ppm, and depend on soil types and land management (Abdel-Sabour et al. 2002). Cr toxicity depends on its oxidation status. While Cr3+ is considered relatively harmless, Cr6+ is highly toxic. Cr uptake can cause diarrhoea, bleeding in the stomach and intestines, liver and kidney damage and cramp. Nickel (Ni) compounds are relatively non-toxic for plants and animals, but there is an increased risk of respiratory tract cancer, due to exposure to nickel sulphide and oxides (Sundermann, 1991).

Zheng (2006) conducted similar study in Franklinian basin, North Greenland. Rather than detecting mineral deposits with SMF, the study implemented the Mixture tuned Matched Feature (MTMF) using same imagery combination of Landsat 8 and ASTER satellite data. By monitoring the spectrum responses of tailings to arsenic (As) and lead (Pb) concentration, (He, Jia 2004) employed RS to study the chemical composition,

mineralogy, and spectral properties of the tailings of a hydrothermal gold mine in South Korea.

The study discovered that the shortwave infrared (SWIR) region at absorption sites of the hydrothermal alteration minerals was where the spectral responses related with as and Pb concentrations were found. The detection models, which were statistically significant, were built utilizing spectral bands of the hydrothermal alteration materials' absorption characteristics. Between the tailings and the soils in the mining area, there are clear changes in spectral properties and spectral responses to heavy metal contamination, according to the study. While the hydrothermal alteration minerals in tailings were linked to spectrum signals to heavy metal concentration, clay minerals from weathering processes were responsible for those in the soil in mining areas. The study concludes that the primary regulating elements of spectrum responses to heavy metal contamination are geological processes related to the creation of soils and tailings. Although, this study presents the closest idea to detection of Pb tailings/pollution in top soil, the study was not able to precisely identify the specific spectral signature for mapping Pb pollution in soils. Moreover, the study did not present any model for determination of soil Pb index.

2.4.1 Detection and monitoring of lead polluted soil

Soil is the heart of agriculture. It is necessary for all crops grown for food and for animal feed. This valuable natural resource is being somewhat lost to increased erosion. In addition, the massive amounts of man-made waste products, sludge, and other products from new waste treatment plants are also contributing to or creating soil pollution. The health of all living things will be improved by taking herculean management measures to preserve the fertility and production of the soil (Sundermann, & Oskarsson, 1991). Recently, soil heavy metal pollution is attracting numerous attentions, and the demand

for rapid testing and screening heavy metal content of soils increasing. This is tied to the global rise in need for food security traceable to increasing populations.

Lead levels in both children's and adults' blood have increased as a result of lead in soil in inhabited regions. Children that practice hand-to-mouth lead transmission experience serious health issues as a result of lead in the soil. Soil needs to be considered as a potential lead channel to people. People should be informed of the threat it poses and the danger it poses so they can take the necessary safety procedures.

This is a very significant issue that regulators and the public health community should realize in order to enact severe rules to safeguard humans, animals, and the environment from lead contamination. Lead metal contamination of soil is largely related to human activity on it. The most common causes of this type of contamination are the failure of underground storage links, the use of pesticides, the application of contaminated surface water to subsurface strata, the dumping of oil and fuel, the leaching of waste from landfills, and the direct discharge of industrial wastes into the ground. Figure 2.4 shows different sources of soil contamination, removal and effects.
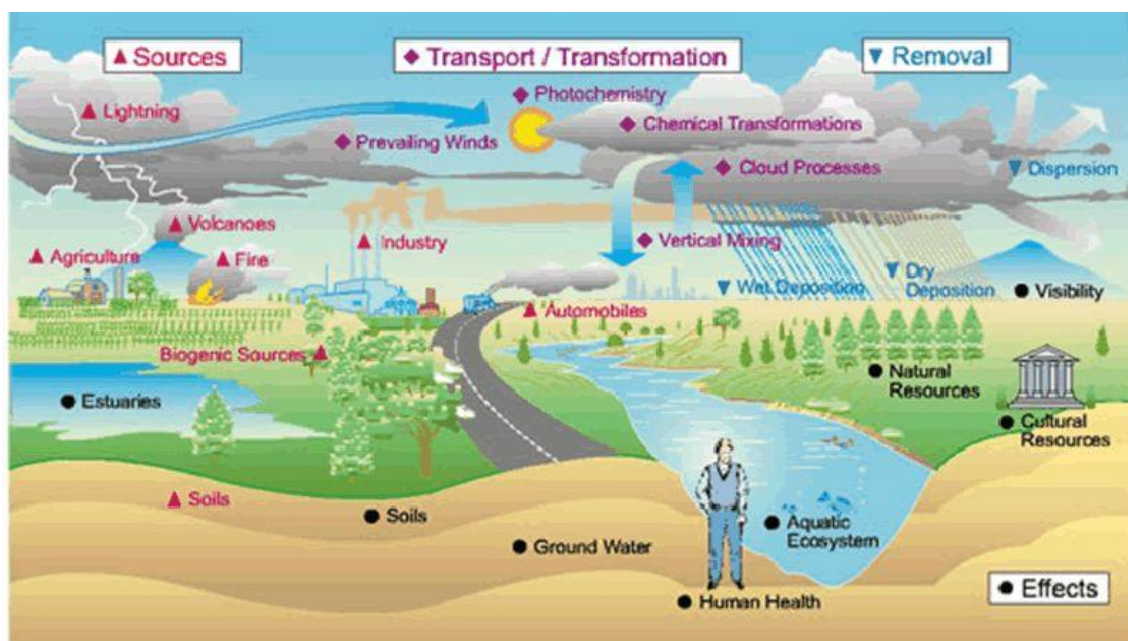
Figure 2.5: Sources of lead pollution (Source: Sundermann, & Oskarsson, 1991)

2.5   Landsat 8 OLI Imageries

Launched in 2013, the Landsat 8 OLI is the new generation of the series of Landsat satellites. It carries two sensors namely OLI (Operational Land Imager) characterized by 9 spectral bands: 4 in the Visible (VIS) (0.43–0.67 mm), 1 band of the Near Infrared (NIR) (0.85–0.88 mm), 2 bands of the Shortwave Infrared (SWIR) (1.57–2.29 mm) and 1 band of cirrus (1.36–1.38 mm) (spatial resolution of 30 m). In addition, it has a Panchromatic band (0.50–0.68 mm) (spatial resolution of 15 m). The second sensor is TIRS (Thermal Infrared Sensor) with 2 bands of 100 m in spatial resolution, operating between 10.60–11.19 mm and 11.50–12.51 mm respectively. Landsat 8 data are characterized by a high radiometric resolution (16 bits), and the scenes cover 180-185 km with a re-visit time of 16days (Lagerkvist, Oskarsson 2007). The images are available at free of charge.

Table 2.2: Band and spatial characteristics of Landsat 8 OLI and Sentinel 2 image

L8 Band		CW (µm)	Wavelength (lower-upper)	Bandwidth	Res. (m)		S2 Band		CW (µm)	Wavelength (min-max)	Bandwidth	Res. (m)
1	C/A	0.443	0.435 - 0.451	0.016	30	C/A	1	C/A	0.443	0.421 - 0.457	0.036	60
2	Blue	0.482	0.452 - 0.512	0.060	30	Blue	2	Blue	0.494	0.439 - 0.535	0.096	10
3	Green	0.561	0.533 - 0.590	0.057	30	Green	3	Green	0.560	0.537 - 0.582	0.045	10
4	Red	0.655	0.636 - 0.673	0.037	30	Red	4	Red	0.665	0.646 - 0.685	0.039	10
							5	VRE	0.704	0.694 - 0.714	0.020	20
							6	VRE	0.740	0.731 - 0.749	0.018	20
							7	VRE	0.781	0.768 - 0.796	0.028	20
							8	NIR	0.834	0.767 - 0.908	0.141	10
5	NIR	0.865	0.851 - 0.879	0.028	30	NIR	8a	NIR	0.864	0.848 - 0.881	0.033	20
							9	WV	0.944	0.931 - 0.958	0.027	60
9	Cirrus	1.373	1.363 - 1.384	0.020	30	Cirrus	10	Cirrus	1.375	1.338 - 1.414	0.076	60
6	SWIR	1.609	1.567 - 1.651	0.085	30	SWIR	11	SWIR	1.612	1.539 - 1.681	0.142	20
7	SWIR	2.201	2.107 - 2.294	0.187	30	SWIR	12	SWIR	2.194	2.072 - 2.312	0.240	20
8	Pan	0.590	0.503 - 0.676	0.172	15							
10	TIRS	10.895	10.60 - 11.19	0.590	100 *							
11	TIRS	12.005	11.50 - 12.51	1.010	100 *							

2.6   Research Issues from Related Works

In the previous section, earlier research attempts to identify Pb concentration in ores and soil pollution were exhaustively discussed. It is seen that while most of the earlier studies have focused on lithological mapping, only few have considered the use of RS for

determination of Pb tailings. Nevertheless, the following facts were identified from the previous literature:

i. Most of the previous studies focused on detection of Pb deposits in ores and rock domes by taking advantage of the known regional characteristics of Pb deposits. However, detection of Pb pollution in soils require a different approach as the concentration of the pollutant is often not significant enough to engender the local geology that were mapped as precursors of Pb presence in most of the previous studies.

ii. Notwithstanding, the studies have identified high positive correlation between Pb presence in soils and spectral irradiation values in the visible portion (VIS) of the electromagnetic spectrum. This justifies the use of satellite imageries containing the visible portion of the spectrum in this study based on the outcome of the previous studies.

iii. Band rationing (BR), Principal Component Analysis (PCA) and Spectral Filtering techniques have been very reliable combination of remote sensing tools for distinguishing spectral signatures of heavy metals. The main advantage of these tools is their ability to highlight certain lithological units of metals based on the spectral capacity of the incident light.

iv. Spectral analysis has usually been done with Landsat 8 OLI and ASTER images. The LandSAT 8 OLI has capacity to sense the visible spectrum (VIS) (0.43–0.67 mm), Near Infrared (NIR) (0.85–0.88 mm), Shortwave Infrared (SWIR) (1.57–2.29 mm) and TIR (Thermal Infrared) (11.50 – 12.51 mm). It has spatial and radiometric resolution of 15m and 16bits respectively (Roy *et al.,* 2014). ASTER images on the other hand have capacity to sense the Visible Near Infra-red (VNIR), Shortwave Infrared (SWIR) (1.57–2.29 mm) and TIR (Thermal Infrared)

(Zheng (2006). Obviously, both satellites sense the VIS and SWIR portions that have been established to be spectral range of response for Pb. However, both images do not have capacity to penetrate the top soil (Lagerkvist, Oskarsson 2007), hence is not efficient for mapping the vertical spread of Pb in the soil. Furthermore, the best spatial resolution achievable by this combination is 22m which also is not suitable for mapping the lateral spread of Pb in any given location.

CHAPTER THREE

3.0   **METHODOLOGY**

This aspect of the research focuses on the procedures or methods that were employed during all stages of the research. It contains data acquisition, data preparation and processing, including how the results obtained were assessed. The final stage of these methods reveals that the aim of the project has been achieved.

Figure 3.1 is a schematic layout of all the stages and procedures implemented in this research.

```
┌─────────────────────────────────┐        ┌──────────────────────┐
│ Hyperspectral remote sensing    │───────▶│ Image classification │
│ data                            │        └──────────────────────┘
└─────────────────────────────────┘                   │
              │                                        │
              ▼                                        │
┌─────────────────────────────────┐                   │
│ Spectral analysis of lead       │                   │
│ tailing in soil                 │                   │
└─────────────────────────────────┘                   │
         │         │                                   │
         ▼         ▼                                   ▼
┌──────────────┐        ┌──────────────────────┐
│ Normalize    │        │ Principal Component  │◀──┘
│ Differential │────────│ Analysis             │
│ Lead Index   │        └──────────────────────┘
└──────────────┘
     │    │
     ▼    ▼
┌──────────────┐        ┌──────────────────────────────┐
│ Mapping of   │        │ Comparative Analysis of NDLI │
│ lead         │        │ and PCA approaches for       │
│ tailings in  │        │ detecting lead tailing in    │
│ soil         │        │ soil                         │
└──────────────┘        └──────────────────────────────┘
     │    │
     ▼
┌──────────────────┐        ┌──────────────────────────┐
│ Geo-location of  │        │ Acquisition of samples   │
│ lead-contaminated│───────▶│ of lead contaminated     │
│ soil hotspots    │        │ soil from field          │
└──────────────────┘        └──────────────────────────┘
     │                                  │
     ▼                                  ▼
┌──────────────────────────┐        ┌──────────────────────────┐
│ Validation of            │        │ Laboratory investigation │
│ applicability of         │◀───────│ of presence of lead in   │
│ geospatial techniques in │        │ soil samples             │
│ mapping lead tailing in  │        └──────────────────────────┘
│ soil                     │
└──────────────────────────┘
```

Figure 3.1: Flow of methods

3.1   Materials and Equipment used

During the course of this study, field and office works required the use of some certain equipment and software.

The research work was majorly dependent on satellite data; however, these data were processed on the computer system and due to the need for ground truthing the outputs, positioning instrument was used. Also, the biological laboratory processing of soil samples also requires that some laboratory equipment be put to use. Table 3.1 shows the list of equipment used in this study and their various purposes they served.

Table 3.1: Equipment used

S/No	Equipment	Purpose
1.	DELL Personal Computer - 4 GB RAM - 465GB Memory - 2.21 GHz Processor - 64bit	For the processing of satellite imageries, processing and analysis of the same
2.	Handheld GPS Receiver Etrex	For locating positions of soil samples mapped to be hotspot of contaminated soil
3.	Cylindrical flask, spatula, among others	

3.1.1 Software used

Table 3.2 contains list of necessary software required for data processing, display and analysis and the purpose to which they were put.

Table 3.2: Software used

Software	Purpose
ArcGIS 10.4	Implementation of band rationing spectral analysis
QGIS	Implementation of PCA
Microsoft word	Report writing
Microsoft excel	Descriptive statistics
CorelDraw	For picture enhancement and merging

3.2 Data Acquisition

This study assessed the applicability of geospatial techniques in mapping lead pollution in soil. The output of the geospatial approaches was tested for their validity using biological laboratory result for detecting lead in soil. Data acquired here have been classified as field data and remotely sensed data.

3.2.1 Acquisition of remotely sensed data

Remote sensing is daily evolving. Several type of remotely sensed data can be used in studying Earth properties, also for assessment of pollutants of soil so far the necessary channels (bands) that reflects the target substance or object were included in the satellite acquiring the images. LANDSAT, SPOT, Sentinel and so on are examples of satellites equipped with the channels (acquiring different bands) that can acquire data about earth features in varied spectral bands. One of the distinguishing differences among these satellites is the resolution of the image they are acquiring (due to the differences in the facilities they are equipped with, the altitude at which they are operating among others). Resolution of satellite images determines the accuracy of the produces from these images. This study employed Landsat 8 OLI which was acquired for two different periods. One of these time series was ensured carries a date within the time of study. This Landsat 8

data acquired has 9 spectral bands and they are all of 30m resolution. Website of the USGS Earth Explorer (www.earthexplorer.usgs.gov) is the source of the datasets acquired.

3.2.2   Acquisition of soil samples from the field

Having mapped out lead metal tailings in soil within the study area, hotspots of lead contaminated soil were marked from the spatial analyst software (ArcMap 10.4) employed in this study, coordinates of these spots were autogenerated. Since these spots were the detected hotspots, it is perfect that their location on the ground should be identified and soil samples taken from these spots. These coordinates of polluted soil hotspots were tracked using the handheld GPS receiver. The positioning satellite receiver (Garmin etrex – handheld GPS) was configured first to select the datum, unit. Clarke 1880 (Minna datum) was selected as the reference datum for the positioning while metre was selected as the unit of the coordinate values. Since it is post-pointing, the position of the sampled crops was typed and each selected and tracked. However, in order to ensure a considerable level of planimetric accuracy, enough satellites were ensured stabilized and observed by the receiver (to observe at 3m horizontal accuracy). Table 3.3 indicates the coordinates of the set-out lead metal hotspots in the study area which are also position coordinates of soil samples tested in the laboratory.

Table 3.3: Post-pointed soil samples location

FID	Id	POINT_X (m)	POINT_Y (m)	Localities
1	0	234597.2061	1065974.528	Maitumbi
2	0	226278.0922	1067527.667	Bosso
3	0	229580.7447	1063439.519	Stadium area
4	0	232768.1253	1064956.033	Maitumbi GRA
5	0	228966.6017	1064975.116	Government Sec.
6	0	231669.0697	1059846.334	Mapi
7	0	229343.2163	1062450.176	Mechanic village
8	0	225503.6996	1065569.943	Dutsen Kura

3.3   Data Processing: Spectral Analysis

Spectral imaging has emerged as a substitute for high-spatial-resolution, large-aperture satellite imaging technologies for remote sensing of terrestrial features and objects. Early uses of spectral imaging and analysis focused on ground-cover classification, mineral exploration, and agricultural evaluation. These applications made use of a restricted number of spectral bands that were carefully chosen and dispersed across the visible and infrared spectrums. There are various techniques by which satellite images can be spectrally processed and assessed for scientific studies. Among the techniques are image classification (for categorizing satellite imagery to different land classes), band rationing (mathematical manipulation of different bands of imageries), PCA, Kaukaff's technique, etc. In this study, the band rationing and PCA approach of spectrally analyzing satellite images were implemented in this study.

3.3.1   Band rationing

An effective method for processing images in remote sensing is band rationing Technique: We divide the DN value of any one band by the value of another band for each pixel. This quotient produces a new set of numbers, most of which are fractional (decimal) values between 0 and commonly 2 to 3 but which may vary from zero (0/1) to 255 (255/1) (e.g., $84/49 = 1.7143$; $109/100 = 0.1090$). Depending on the computer display limitations, we can rescale these ratio values to produce a gray-tone image with up to 16 or 256 levels. Dark shadows are eliminated as a result of ratioing since their values are close to zero in all bands.

This tends to create a more accurate representation of hilly topography because the shaded regions are now depicted in tones similar to the sides that get sunshine. To put it another way, band rationing eliminates shadows. As an illustration, color composites made from three pairs of ratio images that have been co-registered (aligned) are possible. Based on exceptional or abnormal ratio values, several ground features tend to be highlighted in both the individual ratio photographs and these composites. For instance, an ore deposit may weather or undergo other changes that cause the gossan or surface staining to form, which is diagnostic. Hydrated iron oxide (rust), which is often yellow-brown, is what causes this stain. This material has significant red reflection in Band 3 but is likely to be dark in Band 4. Because of this, the ratio quotient values for this scenario frequently surpass 2, leading to a brilliant spot pattern in a 3/4 ratio image.

Division of a band by another gives rise to a satellite output which carries information about the Earth. This information can be of great benefit to the study of the environment. However, these mathematical manipulations have for the purpose they serve been give different name but generally regarded as index. This study formulated its own index that

makes use of different bands of satellite imagery for detection and analysis of lead metals tailing in soil.

3.3.2 Normalized difference lead index (NDLI)

Different colour combination images (CCs) can be used to enhance the existence of lead in the soil at different levels of lead concentration. Specifically, since Pb earlier studies have shown a high spectral reflectance capacity of lead in the visible spectrum, a band ratio of green, red and short wave infrared as shown in equation (3.1) is proposed to enhance the presence of lead for the Landsat 8 OLI as follows:

$$NDLI = \frac{10 \ x \ (Band \ 3 + Band \ 4 + Band \ 6)}{(Band \ 5 + Band \ 6)} \qquad (3.1)$$

3.3.2.1 Implementation of NDLI

In order to map the tailings of lead in soil of the study area, bands of the Landsat 8 OLI were ratioed using equation (3.1). This was implemented using the 'Raster calculator' of ArcMap. Raster calculator is a spatial analyst tool in ArcMap which allows raster images (or bands) to be mathematically combined. The tool creates and implements a map algebra expression that will give a raster output. In doing this, just like in programming, syntax rules of combining the raster datasets using the addition and multiplication operators in the order of equation 3 was followed. This tool can be accessed under the 'map algebra' tool in spatial analyst tab of arc-catalog. The 'rasters' list on the calculator's interface was used in order to select the datasets and variables to use in the NDLI. The 'tools' tab which provides list of commonly used conditional and mathematical operators, allowing easy algebraic expression of the raster bands. Also, the numerical multiplier (10) which is meant to exaggerate the NDLI values was included using the number pane. Figure 3.2 shows the interface of the raster calculator and how the expressions were input in Arcmap.
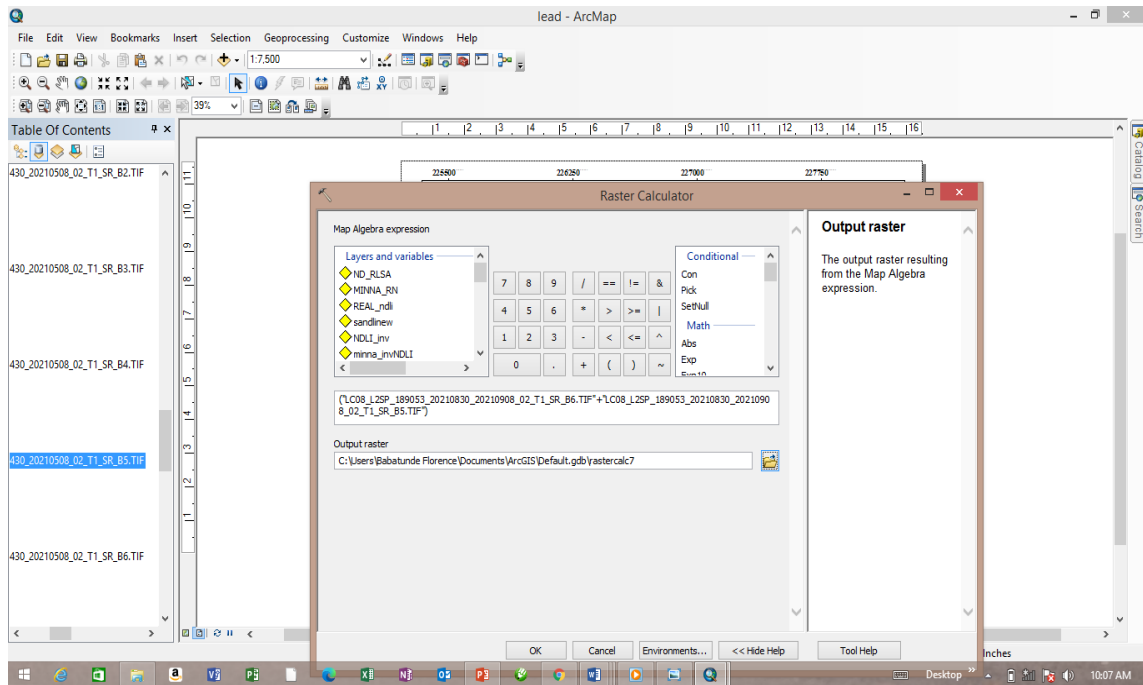
Figure 3.2: Execution of NDLI in ArcMap

3.3.3 Principal component analysis (PCA)

PCA is a multivariate statistical method that chooses uncorrelated linear combinations of variables (eigenvectors) in a way that makes each principal component of the sequentially extracted linear combinations. This method removes data redundancy, isolates noise in the output PC bands, and amplifies some spectral characteristics to stand out from the background. In this research, having employed band rationing approach of processing satellite image bands, for the purpose of detecting lead metals in soil, PCA was implemented. Four bands of the Landsat ETM+ image covering the area of interest were analyzed for the purpose of deducting the principal components, and hence, for detecting and emphasizing the distribution of lead metals across the study area.

3.3.3.1 Steps involve in principal component analysis (PCA)

STEP 1: STANDARDIZATION: These were done to ensure that each continuous starting variable contributed equally to the analysis by standardizing their range.

$$Z = \frac{Value - mean}{Standard\ deviation} \qquad (3.3)$$

49

In the equation given above, Z is the scaled value,

Where

$$Mean = \frac{Sum\ of\ the\ terms}{Total\ number\ of\ terms}$$ (3.4)

$$Standard\ Deviation = \sqrt{\in \frac{(x-mean)^2}{n}}$$ (3.5)

$$x = Value\ in\ a\ data\ set, n = The\ dataset's number\ of\ values$$

STEP 2: COMPUTE THE COVARIANCE MATRIX: They were conducted to determine how the variables in the input data set differ from the mean in relation to one another, or, put another way, to determine whether there is a relationship between them. Since variables can occasionally be highly connected to the point where they contain duplicated data. So, we compute the covariance matrix in order to discover these relationships. The formula of variance can also be written as:

$$Covariance\ matrix = \begin{bmatrix} Cov\ (x,x) & Cov\ (x,y) \\ Cov(y,x) & Cov\ (y,y) \end{bmatrix}$$ (3.6)

Where

$$Covariance = \frac{Sum\ (x-(mean\ of\ x)(y-(mean\ of\ Y))}{Number\ of\ data\ points}$$ (3.7)

STEP 3: COMPUTE THE EIGENVECTORS AND EIGENVALUES: These are the principles of linear algebra that were determined from the covariance matrix to identify the main variables in the data.

STEP 4: FEATURE VECTOR: This phase involved deciding whether to preserve all of these components or toss out any that had low eigenvalues and combine the remaining ones to create a matrix of vectors that we'll refer to as the "Feature vector." Hence, the feature vector is just a matrix with the eigenvectors of the components that were retained as columns.

$$Av = \lambda v$$ (3.8)

then λ is called eigenvalue associated with eigenvector v of A.

STEP 5: RECAST THE DATA ALONG THE PRINCIPAL COMPONENTS AXESThe goal of this final step is to reorient the data from the original axes to those represented by the principal components using the feature vector created using the eigenvectors of the covariance matrix (hence the name Principal Components Analysis). To do this, multiply the original data set's transpose by the feature vector's transpose.

$$Final\ data\ set = Standardized\ original\ data\ set * feature\ vector \qquad (3.9)$$

Image processing software such as ENVI, Erdas Imagine, ArcGIS have PCA tools inculcated in them. ArcMap was used for the graphical and mathematical implementation of the PCA. Arcmap has inherent algorithm of accepting as many bands or layers (raster data) to output a single multiband. For the PCA carried out using Arcmap, the four raster bands (bands 4-6) within the visible spectrum, which has the potentiality of revealing lead tailings in soil were used as the input rasters, the location of the output multiband (raster file with the principal components). For the sake of having a textual output where the eigene vector and other statistical parameters of the PCA are highlighted, the output file was ensured saved with an extension .txt. However, before this execution, the image analysis tool of arcmap was activated using the 'customize' menu bar of the software.
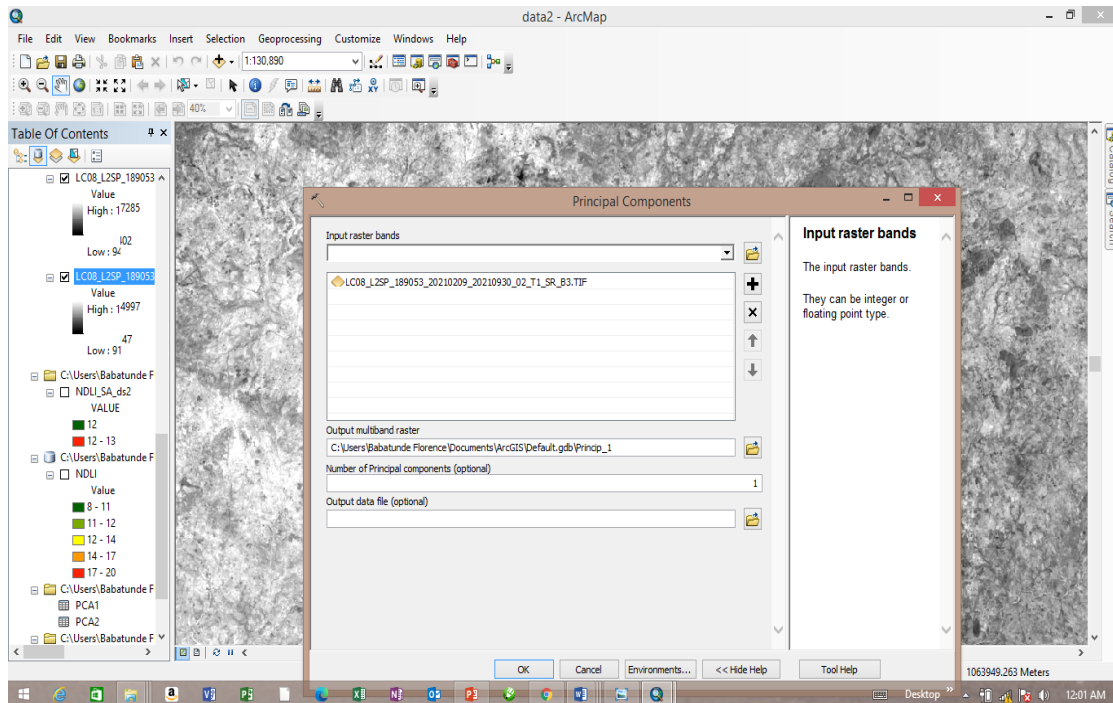
Figure 3.3: Execution of PCA in Arcmap

3.4   Mapping of Lead Tailings in the Soil

The output of the executed NDLI was here manipulated and assessed for the existence of lead in the soil region of the area of study. Also, the PCA outputs were assessed for the tailings of lead metals in the soil.

3.4.1   Lead tailings from NDLI map

For the band rationing output (implemented NDLI), since a multiplicative constant of 10 was included in it, it is expected that the raster cells across the NDLI map should be in tens. In order to enhance the detection of lead in the soil, the symbology tool of Arcmap was used. The colour pallet tab of the symbology was used, ensuring the likely lead hotspot (with maximum NDLI value) are highlighted red. For the sake of testing and validating efficiency of the developed lead index, another Landsat 8 OLI dataset covering the same area (same row and path numbers) but of different time of capture was used. The same process of implementing NDLI as earlier discussed was followed to process the second dataset.

52

Figure 3.4 shows the raster output (with aesthetic and easy to interpret cartographic input) from the NDLI implemented from the dataset.
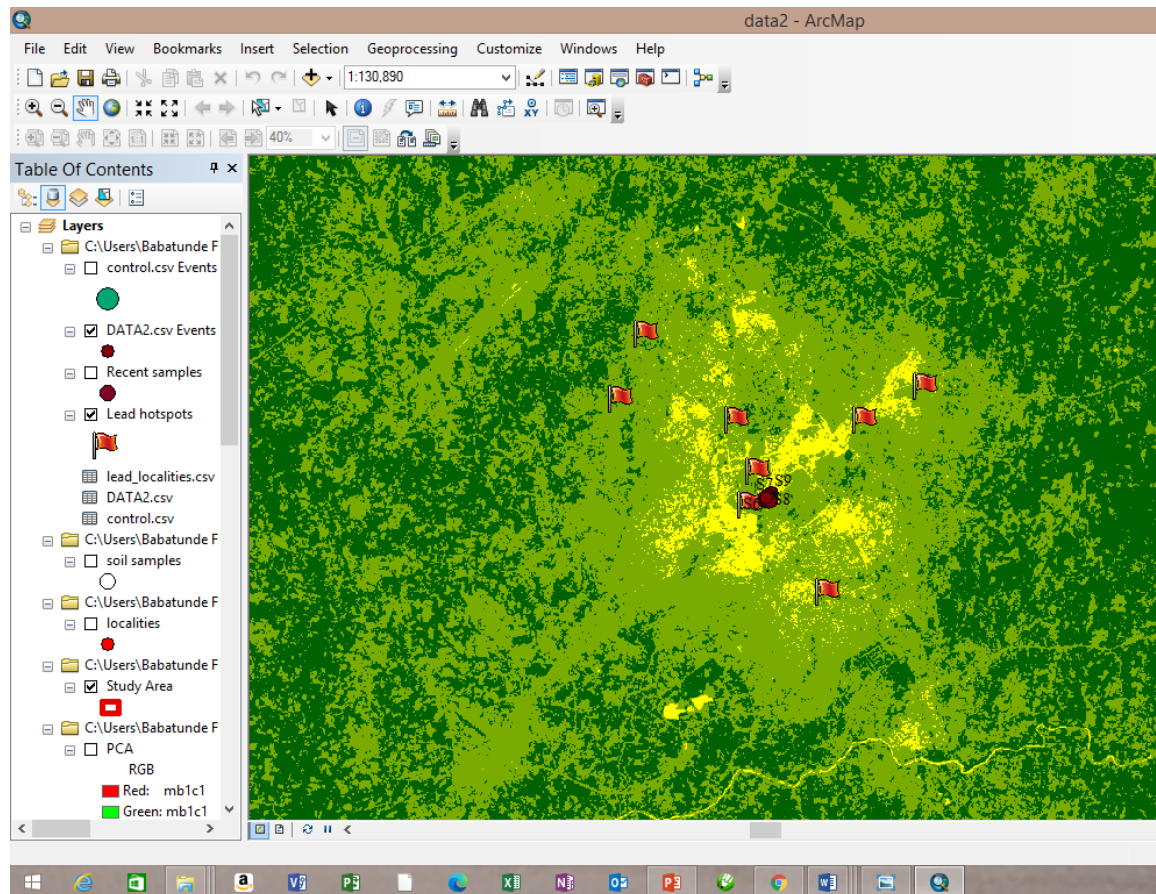
Figure 3.4: Cartography of produced NDLI map

3.4.2   Lead tailings from PCA

The purpose of PCA is to minimize the dimensionality of the input data for spectral analysis (of lead in soil), giving an output of the most useful principal components (raster multiband that carry most information about the target object). Four principal components (PC1 to PC4) resulted from the analysis (synonymous to the number of input raster bands), out of which the PC1 carrying the most information as discussed in chapter four. The three principal components however were assessed to see which of them reflects the presence of lead in soil. There is need for a selective exploration of each of the principal

components. In order to explore the PC1 and PC2 which contains the most amount of information needful for detecting lead metal across the study area, the Eigenevectors of the variance-covariance matrix was analyzed.

Table 3.4: Shows the Eigene-vectors of the variance-covariance matrix

	PC1	PC2	PC3	PC4
1st Band	0.22050	0.41810	0.40434	0.78299
2nd Band	0.45391	-0.72368	0.51977	-0.00981
3rd Band	0.78000	0.04325	-0.61949	0.07715
4th Band	0.37005	0.54736	0.42729	-0.61715

Column of focus for analysis from table 3.1 are basically that of PC1 and PC2 since PC3 and PC4 are to be discarded for containing less than 4% information carried by the composite of these bands.

In the PC2, there is a contrast observable in the signs and values of the PC's coefficients. The coefficient of the original 2nd band (band 5) had a high negative value (-0.72368) while the remaining bands had positive values (0.04325-0.54736). This coefficient in the PC2 was therefore explored for the possibility of detecting lead on the imagery, therefore, this principal component was plotted. Unexpectedly, output raster for PC2 has a correspondence with 2nd band shown in table 3.1 (with negative value). It is deducible that the negative value is an indication of water bodies in PC2 (map to be discussed in chapter four). This therefore implies that PC2 is not carrying obvious information to detect the presence of lead. Due to this, PC1 was likewise investigated and further interpretations made.

PC1 from table 3.5, carries the largest amount of information in the composite band (about 89%). The third band (band 6) of this principal component (as seen in table 3.4), has the highest value (0.78000) other than the other bands with values ranging from 0.2205-0.45391. This interprets that there is high likeliness that band 6 of landsat 8 (SWIR) can be used for mapping the presence of lead in soil. For the essence of visualizing this effect, this component was also mapped to investigate its tendency of depicting the presence of lead across the study area. For the sake of reliability, PC1 with the highest tendency of reflecting the presence of lead metal in soil was compared to the NDLI map.

Table 3.5: Eigenevalues of the variance-covariance matrix

Component	Eigenevalues	Percentage	Accumulative of eigene values (%)
1	6918585.14419	89.4461	89.4461
2	518033.99414	6.6973	96.1434
3	289977.00688	3.7489	99.8923
4	8327.80237	0.1077	100.000

3.5   Comparative Analysis of Band Rationing and PCA Approaches

Geospatial techniques, especially remote sensing principles require that accuracy of implemented techniques should be checked and the reliability of such should be ascertained either by external factor or by repeated observation or measurement. For this purpose, a comparative analysis of the two approaches employed for the mapping of lead tailings in soil (BR and PCA) was performed. For the purpose of checking the reliability and correlation between the two geospatial approaches, the lead tailings mapped by each of the techniques were assessed on the output raster bands. Principles of image

interpretation were employed to detect similarities or differences in the output rasters of the two techniques under study.

Pattern and shape are two out of the seven elements of interpreting image in remote sensing. These elements formed the major basis of comparison between outputs of the two approaches. The spatial distribution of lead tailings on each of the raster outputs (PCA and BR) was vectorized using polygon tool in Arcmap; this involved tracing of boundary of lead tailings. The polygons formed from the vectorized boundary of lead tailings were compared and a total conformity was noticed on the two raster bands. Also, the locations of these vectorized polygons (on both the NDLI and PCA map) are almost the same. This is the third element of image interpretation employed in the comparative analysis of the output raster. This imply that the two raster from the two techniques carry the same information, hence, increasing the reliability of the geospatial techniques to have been able to detect lead metal in soil of the study area.

3.6 Geolocation of Lead-Contaminated Soil Hotspots

For the purpose of ground truthing (activity of verifying remote sensing data or results from remotely acquired images by comparing it with what exists on the Earth object or phenomenon under study) the output of geospatial technique, detected lead hotspots in soil of the study area were pin-pointed on the NDLI map. Locations or raster cells with the highest NDLI value (values ranging from 17-20) are here referred to as lead hotspot. Points within this raster cells were digitized and the 'add XY' tool on Arcmap was used to generate their coordinates. There were 8 locations visually detected to be lead hotspots in the study area (as contained in table 3.6). For easy tracking of these points on the ground, the locality where each of these hotspots exist were mapped.

Table 3.6: Positions and localities of lead hotspots

FID	Id	POINT_X (m)	POINT_Y (m)	Localities
1	0	234597.2061	1065974.528	Maitumbi
2	0	226278.0922	1067527.667	Bosso
3	0	229580.7447	1063439.519	Stadium area
4	0	232768.1253	1064956.033	Maitumbi GRA
5	0	228966.6017	1064975.116	Government Sec.
6	0	231669.0697	1059846.334	Mapi
7	0	229343.2163	1062450.176	Mechanic village
8	0	225503.6996	1065569.943	Dutsen Kura

3.7   Collection of Samples of Soil Mapped as Lead Hotspot

Soil samples mapped as lead hotspot were collected from the eight (8) locations in table 3.6. In doing this, hand held GPS was used to track these locations with the aid of the coordinate positions. However, the reference datum (Clarke 1880 – Minna datum) with which the NDLI map was produced was the datum set on the hand-held GPS. This is to avoid positional inaccuracy that may be posed due to differences in reference datum of geolocation on map and post-pointing on the ground. Noteworthy, while collecting the sample soil, the following cautions were taken:

    i.   though lead is heavy and can always penetrate into depth of soil, it is still advisable that when collecting samples, the upper or top soil should be collected. Hence, the upper 1-2inches of the soil were collected as sample. It is however, advisable also that in disturbed soil regions, as well as in flowerbeds and vegetable gardens, soil samples should be collected at 6-inches depth.

ii.   a soil auger or corer is the de-factor for fetching the soil from the ground, in the absence of this, a metallic tool that could dig down the soil was used

iii.   the collected soil samples were put and enclosed in a clean container

iv.   before put to use in the lab, wet soil samples were ensured air-dried

3.8 Conventional Method of Laboratory Investigation of Lead (Pb) Test in Soil Sample: Instrumentation

The following are the equipment used in the laboratory for the experimental assessment of the collected soil sample:

Table 3.7: Laboratory equipment

S/No	Equipment	Purpose
1	Hand-held X-ray fluorescence (XRF) analyzer	For quantitative measurement of soil and its analysis
2.	Benchtop stand	For carrying XRF
3.	Siever	For sieving the collected soil samples
4.	Stirrer	For stirring the soil while oven-drying

3.8.1 Sample collection and extraction

There are various steps involved in gathering samples for this study, including selecting the place where the sample will be obtained and gathering the soil sample there.

At each sampling location, soil samples will be gathered from each point. The ring sample method is used during the sampling process. The goal of a ring sample is to collect soil samples for laboratory analysis using a ring soil sampling equipment with a length of around ±20 cm.

Prior to sampling, the soil surface is flattened and cleared of any grass or debris. The sampling ring is then placed perpendicular to the ground surface and pounded with a tiny beam so that it seems to enter the ground uniformly. The soil is then dug to a specific depth (10 cm–20 cm) surrounding the area to insert the sampling ring device. After that, a shovel is used to dig out the sampling ring tool that has penetrated the earth surface. Lastly, the dirt inside the sampling ring is transferred into a plastic sampling bottle container. Soil samples in the plastic container are ready to use.

3.8.2   Sample preparation

The preparation of the sample prior to a laboratory analysis was the study's next stage after sampling. The extraction of soil samples using an acid digestion extraction method (wet digestion) with Aqua Regia solution is the first stage of sample preparation in this investigation.

3.8.3   Wet digestion of soil for the determination of Total Pb, using Atomic Absorption Spectrophotometric (AAS), Procedures.

The total Pb metal concentrations in soil samples are calculated using acid-digestion or wet-digestion extraction. The Aqua Regia acid solution is used in this extraction process. Strong concentrated hydrochloric acid (HCl) and concentrated nitric acid (HNO3) are combined in a 3:1 ratio to create the solution known as aqua regia.

The process of extraction by acid digestion (Wet-Digestion) starts from

i.   Weigh 0.2 - 0.5 grams of soil sample into a 100ml volumetric flask

ii. Add about 30ml of wet digestion acid (carefully measure 650ml of Nitric acid into a 1000ml beaker, add 80ml of Perchloric acid and subsequently, 20ml of sulfuric acid, stir to mix properly

iii.   Place sample on a fume cupboard and digest until sample reduce to 20ml volume. Continue heating until white fumes of Nitric acid disappear and sample reduce to 10ml volume, care must be taken, not to allow sample to dry to avoid loss of sample

iv.   Transfer quantitatively to a 50ml volumetric flask and make to streak with water that has been distillated

 v.   Shake vigorously and filter through a what man 0.45um filter paper

vi.   Pipette 1ml of the clear digest into another 50ml volumetric flask and make to mark with distilled water

vii.   Read samples using AAS (AA WIN 500 PG INSTRUMENT) with appropriate wave length and element parameters

3.8.4   Interpretation (Richard, 2010 – Pennsylvania University)

According to laboratory test results, soil lead concentrations are typically given in terms of µg/g (micrograms per gram), mg/kg, or ppm (parts per million). All of these units of measurement are interchangeable. The level of lead contamination indicated by various soil lead concentrations is shown in table 3.8 below.

Table 3.8: Soil Level of Lead Contamination

Soil Lead Level (Total Sorbed Lead Test)	Level of Lead Contamination mg/kg or ppm
Less than 150	None to very low
From 150 to 400	Low
From 400 to 1000	Medium
From 1000 to 2000	High
Greater than 2000	Very high

3.9   Validation of Applicability of Geospatial Techniques in Mapping Lead Tailing in Soil

For validation of the geospatial technique as an approximate and refined replacement for rigorous and time-consuming laboratory approach of testing for lead metals in soil, a statistical analysis was performed by comparing the NDLI values of lead hotspots with their corresponding ppm output from the laboratory. This statistical testing also reveals the presence of any significant differences between the two approaches under study (geospatial and biological). There are various statistical tests with their peculiarity to different analysis (though there is mutuality), such as chi-square, Analysis of Variance (ANOVA), student's t-test, Fisher's test (F-test), etc., hence, the need to ascertain which befits the analysis. Having decided the befitting test for the analysis, before any test is carried out, null hypothesis H_o would be set and it is alternative H_i. Another key element of statistical testing is the level of significance and its opposite – level of confidence. Level of significance ($\propto$) is the probability of rejecting a null hypothesis by the test when it is really true while level of confidence (c) refers to the probability of a parameter that lies within a specified range of values. Null hypothesis would be rejected when the p-value less than or equal to the level of significance and the reverse is the case for a compliment.

CHAPTER FOUR

4.0   RESULTS AND DISCUSSIONS

4.1   Normalized Lead Index Map of the Study Area

4.1.1   NDLI map from dataset

The developed model (NDLI) which utilizes satellite image bands captured in the visible regions of the EM Spectrum as mathematically stated in chapter three was implemented over Landsat 8 OLI imageries. As a means of testing the reliability of the developed NDLI model, two datasets were used to implement the model, for mapping lead tailings in soil of the area of interest.

Figure 4.1 shows the NDLI map of the study area produced from Landsat 8 OLI image (first dataset) captured by the Landsat 8 within 30th of April, 2021 to 06th of May, 2021.
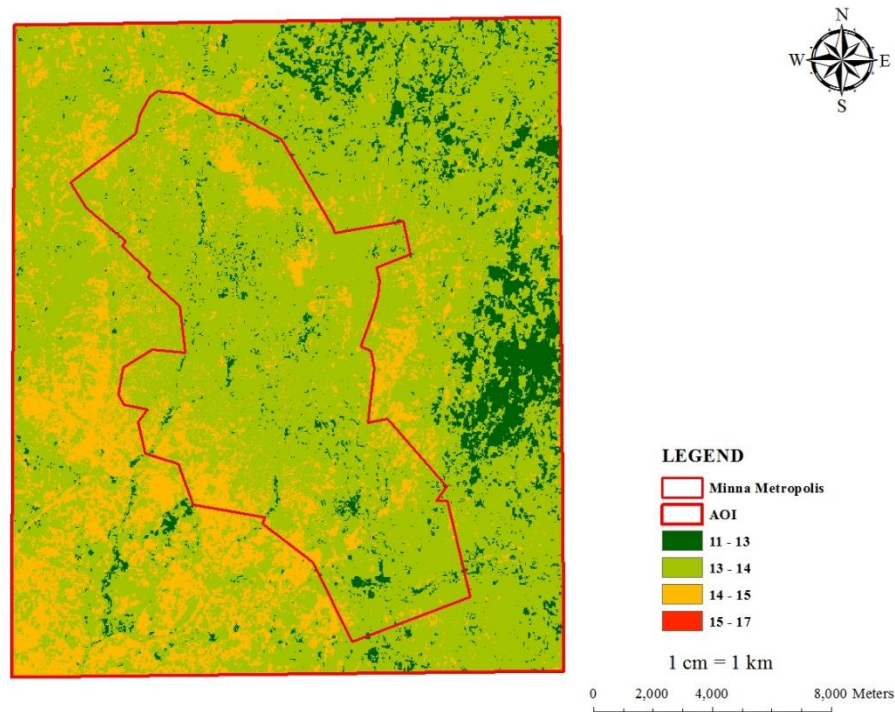

Figure 4.1: NDLI map of area of interest

The NDLI value within the study area ranges from 11 to 17, which has been reclassified into 4 classes of varied intervals (1 and 2). This value range however implies that the NDLI was in a multiple of 10, which is the multiplicative constant in the NDLI model

developed and expressed in chapter three. Obviously, as expected, there are presence of lead across the study area (since lead naturally occurs and found to be minimal in our immediate environments if not deattenuated by anthropogenic activities). The rectangular red boundary is the extent of focus in this study which contains Minna metropolis (boundary shown in red with lighter thickness). Eastern region of the AOI is seen to contain less amount of soil while the South-West region contains relatively higher amount of lead (14-15). Table 4.1 shows the spatial positions (coordinates and their locality) as extracted from Arcmap of the lead hotspots mapped by the NDLI model.

Table 4.1: Lead hotspots positions and localities

FID	Id	POINT_X (m)	POINT_Y (m)	Localities
1	0	234597.2061	1065974.528	Maitumbi
2	0	226278.0922	1067527.667	Bosso
3	0	229580.7447	1063439.519	Stadium area
4	0	232768.1253	1064956.033	Maitumbi GRA
5	0	228966.6017	1064975.116	Government Sec.
6	0	231669.0697	1059846.334	Mapi
7	0	229343.2163	1062450.176	Mechanic village
8	0	225503.6996	1065569.943	Dutsen Kura

However, lead polluted soil hotspots (with red and small raster cells) are seen across the study area, mostly within Metropolis. Because of their fewness and not spreading too largely across the area, these hotspot zones are not visibly seen on the map in figure 4.1 (due to smallness of the scale). To exaggerate these hotspots, lead hotspot thematic map of each of the localities with lead polluted soil were mapped on Google Earth image acquired with SAS Planet. This is needful for the purpose of evaluating the

anthropogenic activity(ies) that might have increased the concentration of lead metal in these lead polluted soil hotspot locations.
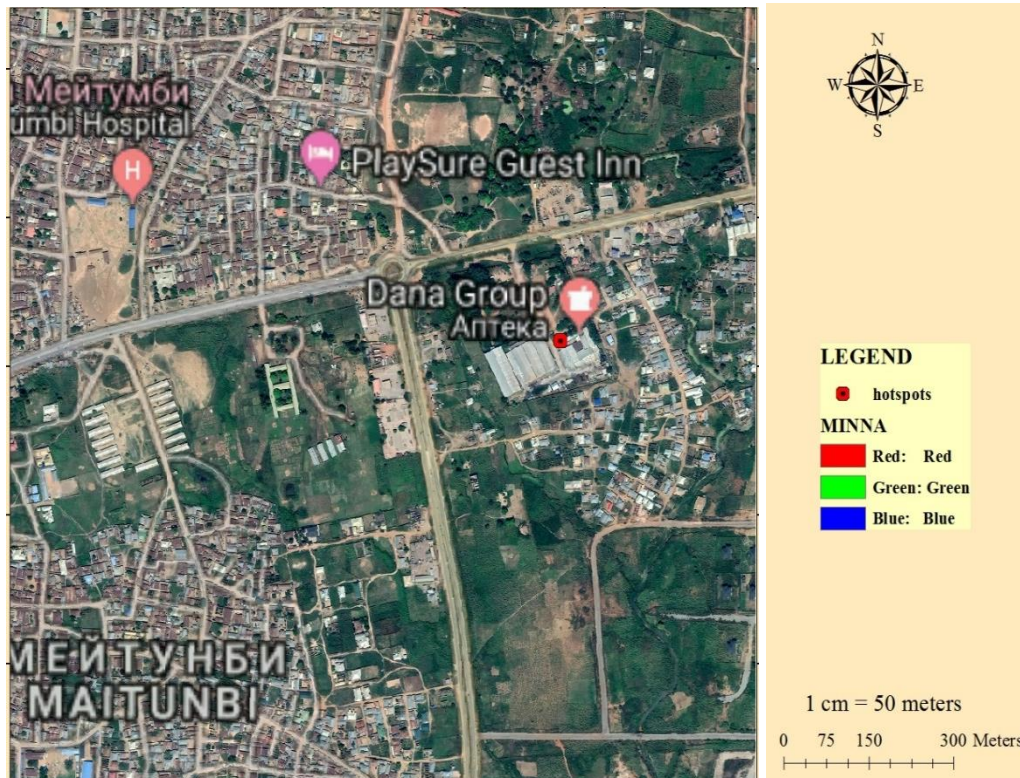
4.1.2.1 Maitumbi

Figure 4.2: Maitumbi hotspot map of lead-polluted soil

Figure 4.2 shows the location of soil detected by the NDLI to contain lead metal within Maitumbi. The hotspot mapped here is around Dana Group, Maitumbi. There is a likeliness that the soil within this location has been polluted due to activities of the Dana Group. This hotspot is likewise around industrial region of Matumbi, since soil can be transported (naturally by some agents including water, wind or storm), Ground truthing however, will be done to validate the presence of lead in the location.
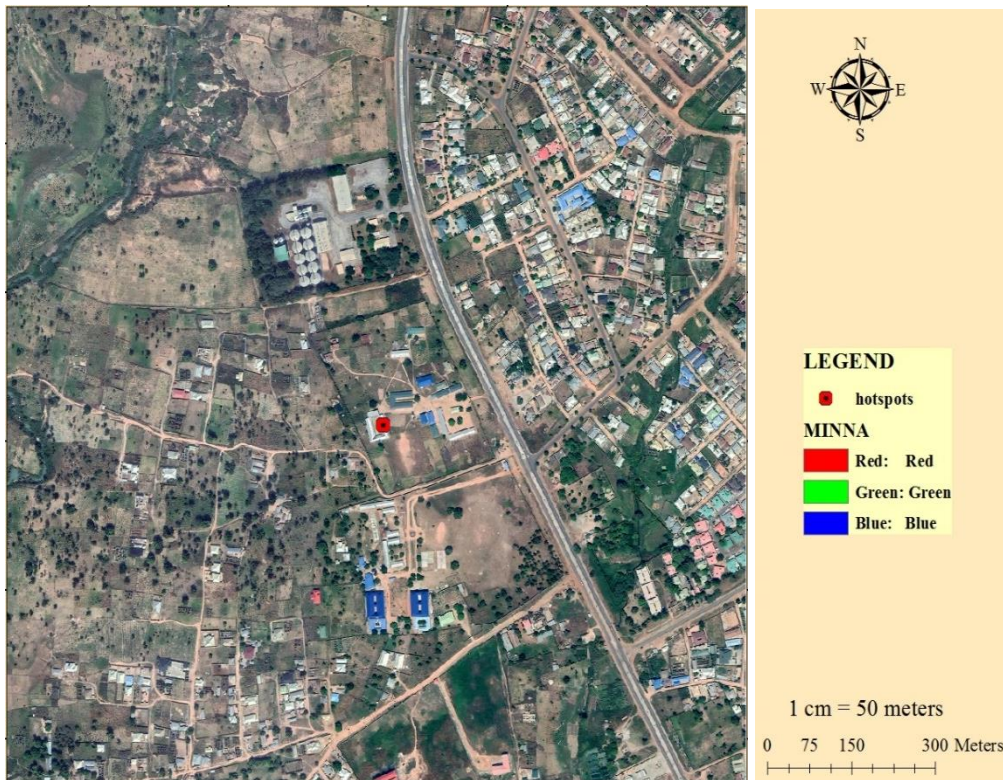
4.1.2.2 Bosso

Figure 4.3: Bosso hotspot map of lead-polluted soil

Figure 4.3 shows the spatial distribution of land use and land cover (on image truth to life) around the lead-polluted soil hostspot in Bosso. Though there are few built up areas in short distance circumference of this hotspot, an industry is located around this region. The likeliness of the increase in concentration of lead in soil in this mapped location however may be traceable to the activities (industrial and manufacturing) that has been happening in and around the location.

4.1.2.3 Stadium area

As seen in figure 4.4, the mapped lead hotspot is within the Stadium area of Minna City, Niger State. This region of the area is seen to be close to a structure, most recently built in this facility area. Smelting activities (involve use of metals) might have been the major cause of the increased concentration of lead, compared to other regions of the facility. This however will be validated through ground truthing.

Figure 4.4: Stadium hotspot map of lead-polluted soil

4.1.2.4 Maitumbi GRA

The Government Reserved Area in Maitumbi was mapped to contain regions of lead-polluted soil in the area of interest considered by this study. The soil region with high concentration of lead in this location was found around densed vegetation. Lead in soil of vegetative area, may be due to proximity of such vegetative region to road, movement of soil due to some agents (including wind and erosion). Edible crops in a vegetation with detected high level of Pb metal are advised not to be consumed, as this may be a source of intake of the metal, known to be poisonous.

Figure 4.5: Maitumbi GRA hotspot map of lead-polluted soil

4.1.2.5 Government Secretariat

The northern region of Minna Government Secretariat was seen to contain soil polluted with lead metal. As seen in figure 4.6, though the map is not suggesting any likely cause of the increased in concentration of lead in this location, this will rather be investigated during the ground truthing and the truthfulness of this also confirmed with AAS test.
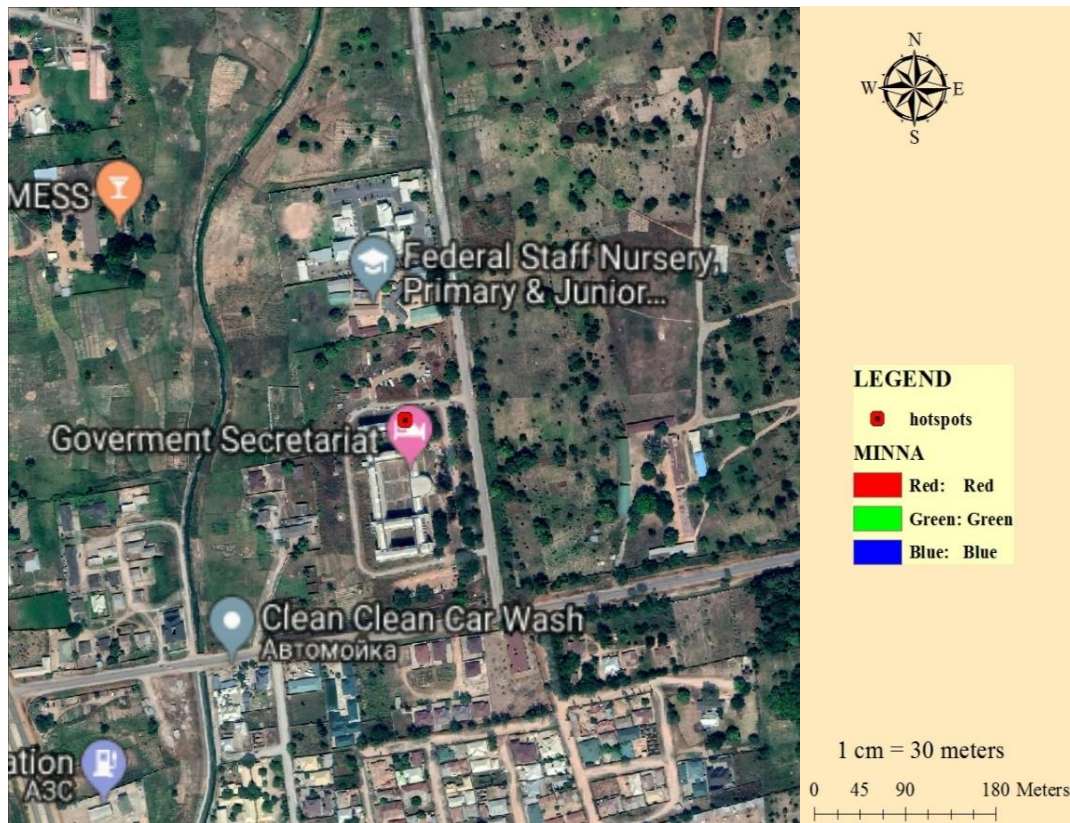
Figure 4.6: Government Secretariat hotspot map of lead-polluted soil

Lead hotspot in this region (seen in figure 4.7) was found behind a religious centre but close to a business district, with lots of production centres in the region. This location of highly lead-contaminated soil is seen along the road that leads to the business district. This hotspot may be due to dispersal of lead metal from waste and other lead source from activities daily carried out in this locality.

Figure 4.7: Mapi Secretariat hotspot map of lead-polluted soil

4.1.2.7 Mechanic village

This lead hotspot is seen within the Mechanic village, Kpakugun. Mechanic village as the name implies is known for mechanical repairs of vehicles. Activities in this location has a high te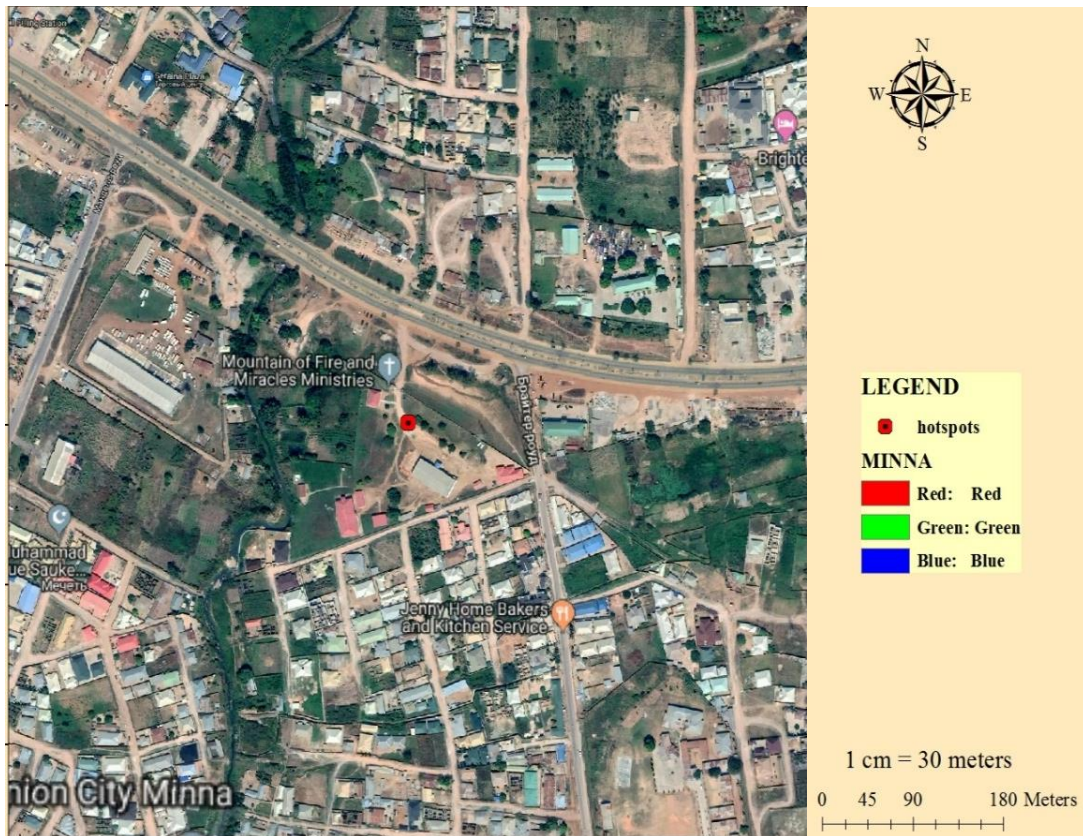ndency of increasing the concentration of lead metal in the soil of this surrounding. Studies (Adewole & Alysius *et al.,* 2013; Abidemi, 2011) have established that auto-repair workshops engage in activities capable of polluting their host surrounding (soil) with heavy metals including lead. In a mechanic shop, there are professionals who work on the engine, the steering and brakes, the spray painting, the charging of the car batteries, the welding, and the soldering, etc. which each generates different types of waste (engine oil and paint, gasoline, diesel, among others), disposed of within the environment, hence, increasing the concentration of lead metal in this location.

Figure 4.8: Mechanic village hotspot map of lead-polluted soil

4.1.2.8 Dutsen Kura

Figure 4.9 shows the location of soil polluted (as mapped by NDLI) by lead metal within Dutsen Kura, Minna. This location is seen some distances away from dispersed settlements in this location. Suggestively, the increase in lead concentration in this location may be as a result of its use as a landfill; where wastes, capable of decaying and polluting the soil with heavy metals such as lead (Pb). However, in order to validate such assumption as this, the site was visited and soil sample collected for laboratory verification of this approach.
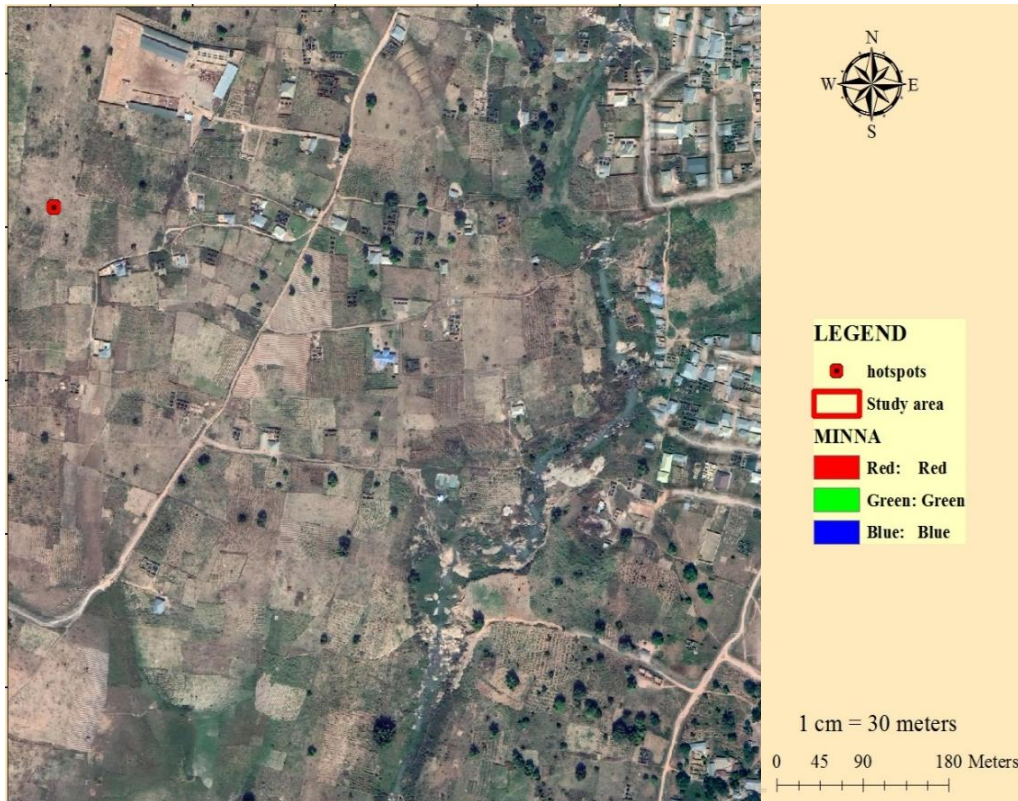
Figure 4.9: Dutsen Kura hotspot map of lead-polluted soil

4.2   NDLI Map from Second Dataset

For the purpose of verifying the results obtained from the implementation of NDLI,

another Landsat dataset, however of different date of acquisition was used to map the

tailings of lead metal within the same area of interest. Figure 4.10 shows the general

NDLI map of the area of interest, with map of Minna Metropolis overlaid on it,

produced using Landsat 8 OLI bands dataset with the attribute (metadata) contained in

table 4.2 below.

Table 4.2: Metadata of Landsat 8 OLI image used as second dataset

S/No	Attribute	Details
1.	Name	LC08_L1TP_190053_20210624_20210630_02
2.	Date of Acquisition	2021-06-24 to 2021-06-30
3.	Path	190
4.	Row	53
5.	Number of bands present	Nine (9); band 1 to 7, 10 and 11

Figure 4.10: NDLI map from second dataset

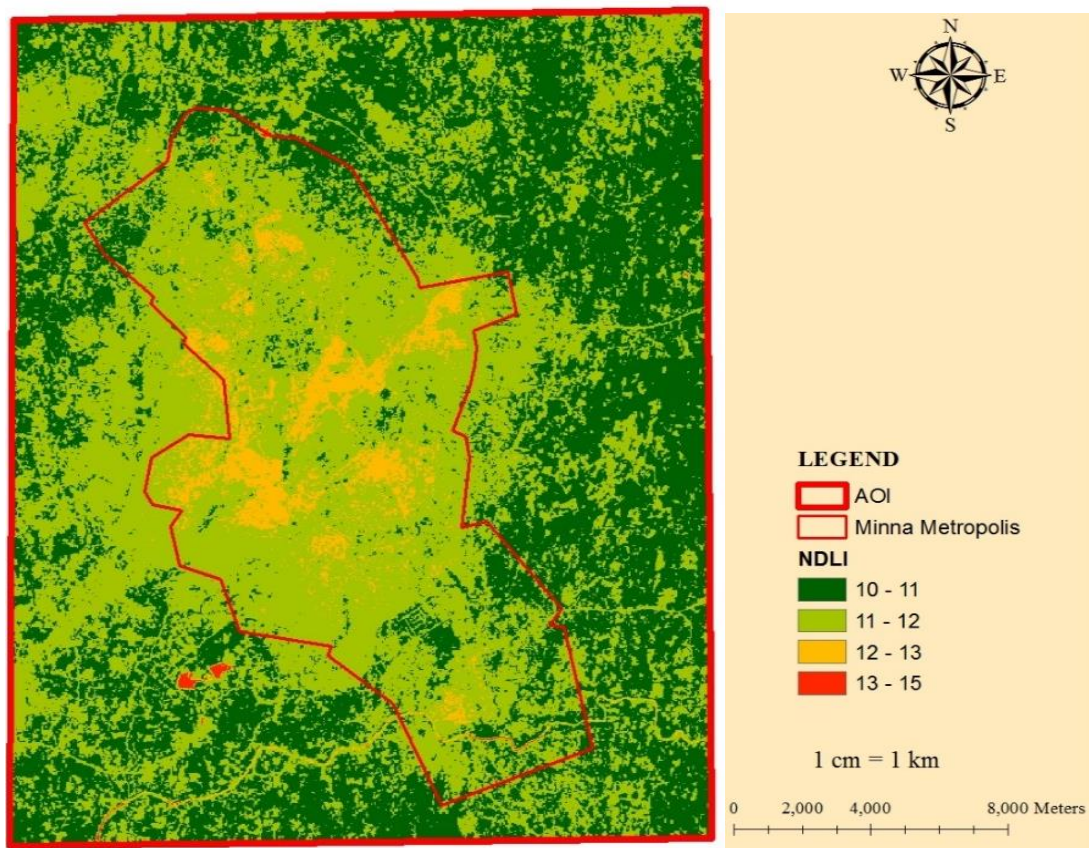The map seen in figure 4.10 shows that high lead concentration (12-13) in June are largely seen within Minna Metropolis contrary to April when we have a minimal spread of lead in the Metropolis (where industrial activities are densest). Outskirt of the Metropolis, lead

pollution in the soil are minimal (or unharmful), contrary to April (as mapped in figure 4.1). The second dataset was captured during the raining season (when rainfall is heavier, compared to April). Soil regions outskirt of Minna Metropolis (seen in April NDLI map) are now covered by vegetation, hence, the index implemented map these vegetative regions to contain the least concentration of lead metal. Also, the NDLI value during this time has reduced from 10-17 (seen in April, 2021) to 10-15 in June, 2021 (which is the time of carrying out this study), hence, water (rainfall) has an effect on the concentration of lead metal in soil. Chemistry explains that when lead (in soil) are soaked in water, the metal's solubility increases and becomes more mobile. Also, they (metals such as lead) can become locked up in bottom sediments (subsurface soil) where they can remain for many years. Hence, the top soil has been washed by erosion (moving water) and the concentration of lead in the soil reduced, possibly transporting them to surrounding water channels. As seen in the map (figure 4.10), water bodies in the south-west region of the study area was detected to contain high level of lead metal. This is however expected, since lead in water are majorly sourced from dispersal of lead metal from waste in non-aquatic region of an area. Nonetheless, there are other soil land covers within the area of interest with highest level of lead pollution (13-15). To investigate if the soil mapped in the earlier dataset as hotspots (contained in table 4.1) are still highly polluted with lead metal, these locations were overlaid on figure 4.10.

4.2.1   Hotspot map of lead-polluted soil from the second dataset

Figure 4.11 shows the hotspot map of lead-polluted soil within the study area. These locations overlaid on the map all have NDLI value within 13-15. This ascertain that soil in these localities are indeed highly polluted with toxic lead metal. On the second dataset, the extents (their spread) are seen to have reduced compared to that of the first dataset, traceable to the weather condition during this period.
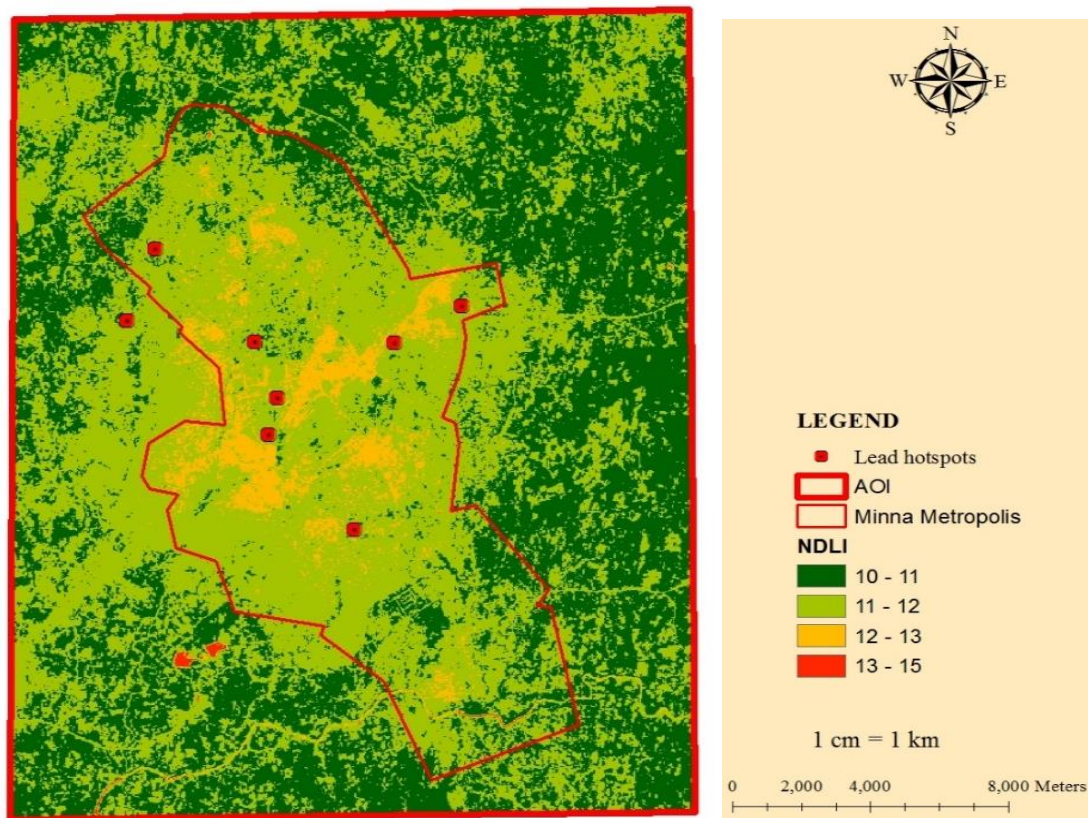
Figure 4.11: Hotspot map of lead-polluted soil from second dataset

4.3   Principal Component Analysis

4.3.1   Variance-covariance matrix of PCA

Table 4.3 shows the Eigene values of the variance-covariance matrix output by the PCA

Table 4.3: Eigene values of the variance-covariance matrix

Component	Eigenevalues	Percentage	Accumulative of eigene values
1	6918585.14419	89.4461	89.4461
2	518033.99414	6.6973	96.1434
3	289977.00688	3.7489	99.8923
4	8327.80237	0.1077	100.000

Table 4.3 shows the eigenvalues of the four components (the extracted linear combination of the bands) from the PC analysis performed. Component 1 (PC1) however carries the largest amount of information (about 89%) followed by the second component (PC2)

74

which carries about 7% of the information in the four bands (ratioed or combined). Therefore, the last two components (PC3 and PC4) could be discarded as they both merely carry 4% of information from the image channels.

This output in table 4.3 implies that PC1 and PC2 carry the most information that can be needed from the input layers or bands. Hence, these two components were expected to have the least amount of correlation; since PCA is aimed at discarding components which may carry the same amount and kind of information as some other components (just as PC3 and PC4 are here discarded and are expected to have higher correlation values with themselves and also with PC1 and PC2). For validation of this proposition, table 4.4 shows the correlation matrix of the four components.

Table 4.4: Correlation matrix

	PC1	PC2	PC3	PC4
PC1	1.00000	**0.64669**	0.78306	0.97827
PC2	**0.64669**	1.00000	0.84483	0.71216
PC3	0.78306	0.84483	1.00000	0.86340
PC4	0.97827	0.71216	0.86340	1.00000

From table 4.4, it is obvious that PC1 and PC2 are the only pair-components that has the least correlation, hence, carry the least similar information. This is another reason for which PC3 and PC4 were hereafter discarded in the analysis.

In order to explore the PC1 and PC2 which contains the most amount of information needful for detecting lead metal across the study area, the Eigenevectors of the variance-covariance matrix was analyzed.

Table 4.5: Eigenevectors of PCA's variance-covariance matrix

	PC1	PC2	PC3	PC4
1st Band	0.22050	0.41810	0.40434	0.78299
2nd Band	0.45391	-0.72368	0.51977	-0.00981
3rd Band	0.78000	0.04325	-0.61949	0.07715
4th Band	0.37005	0.54736	0.42729	-0.61715

Column of focus for analysis from table 4.5 are basically that of PC1 and PC2 since PC3 and PC4 are to be discarded (from table 4.3 and table 4.4) for containing less than 4% information carried by the composite of these bands. In the PC2, there is a contrast observable in the signs and values of the PC's coefficients. The coefficient of the original 2nd band (band 5) had a high negative value (-0.7268) while the remaining bands had positive values (0.04325-0.54736). This coefficient in the PC2 was therefore explored for the possibility of detecting lead on the imagery, therefore, this principal component was plotted.

The output raster for PC2 as shown in figure 4.12 has a correspondence with 2nd band shown in table 4.5 (with negative value). It is deducible that the negative value is an indication of water bodies in PC2 (as highlighted with blue polygon in figure 4.12), though there are traces of a substance within Minna Metropolis but not clear in appearance. This therefore implies that PC2 is not carrying obvious information to detect the presence of lead.
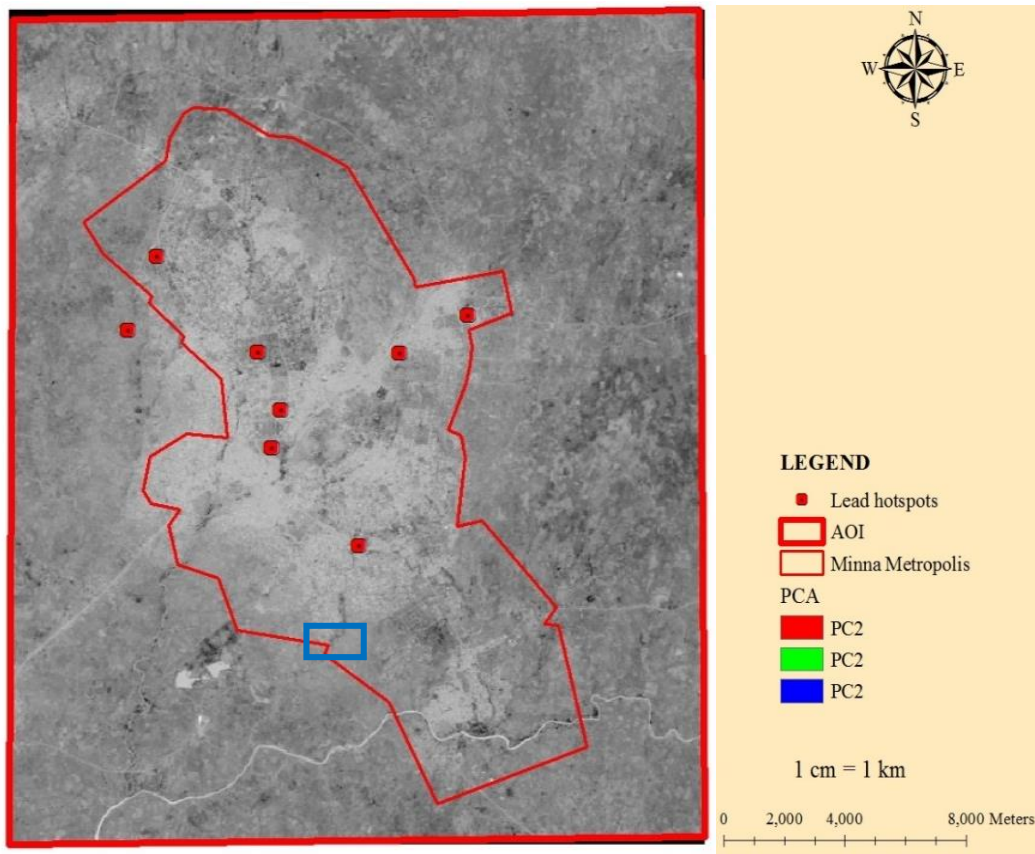
Figure 4.12: PC2 map representation

PC1 from table 4.3, carries the largest amount of information in the composite band (about 89%). The third band (band 6) has the highest value (0.78000) other than the other bands with values ranging from 0.2205-0.45391. This interprets that there is high likeliness that band 6 of Landsat 8 (SWIR) can be used for mapping the presence of lead in soil. For the purpose of visualizing this effect, this component has been mapped to investigate its tendency of depicting the presence of lead across the study area.
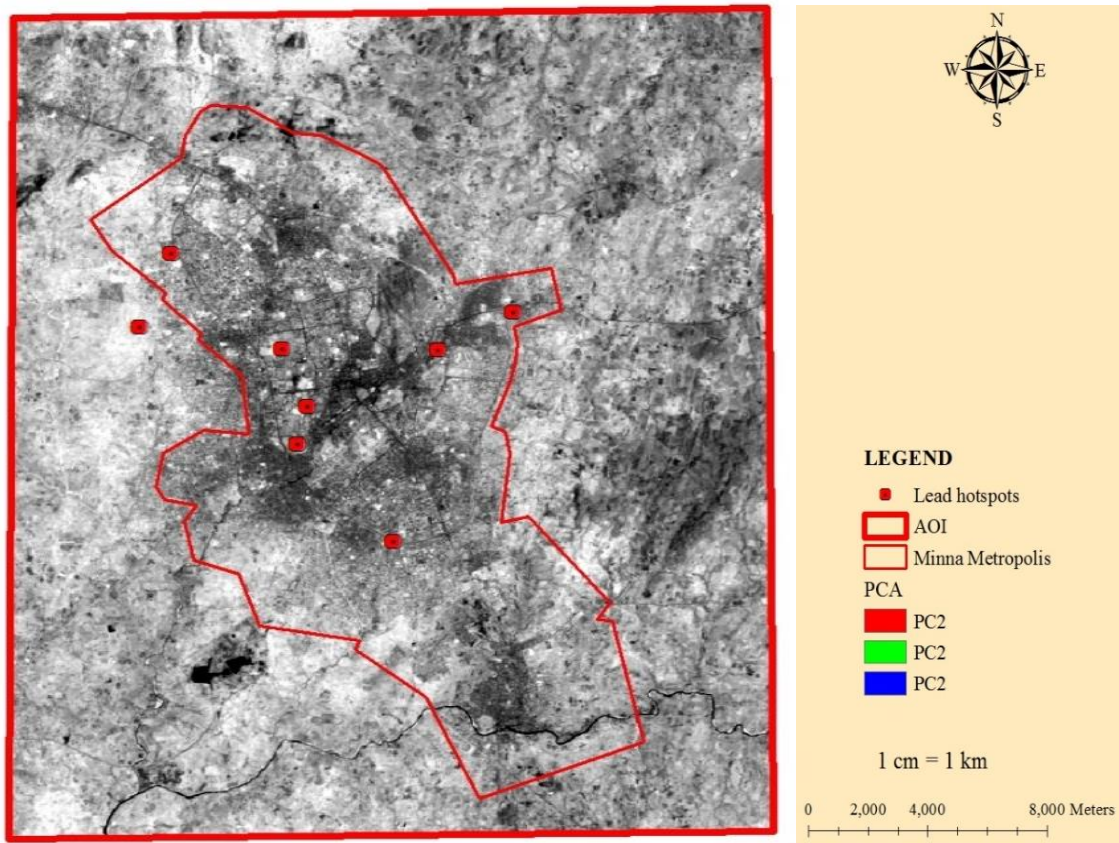
Figure 4.13: PC1 map representation

Figure 4.13 (PC1) has 'very dark' region, 'dark', 'white' and 'grey' regions. The very dark obviously are water bodies in the study area. The dark areas however show the same pattern as the lead polluted areas on NDLI map shown in figure 4.11. This therefore means that PC1 is enough to map out the presence of lead in soil in our area of interest. To clearly see the similarity between the NDLI map (in figure 4.11) and the PC1 map (in figure 4.13, found to be the component enough to map lead tailings in soil), basic elements of interpretation of images (in Photogrammetry and Remote Sensing) were used based on figure 4.14.

4.4 Comparative Analysis of Band Rationing and PCA Approaches for Detecting Lead Tailing in Soil
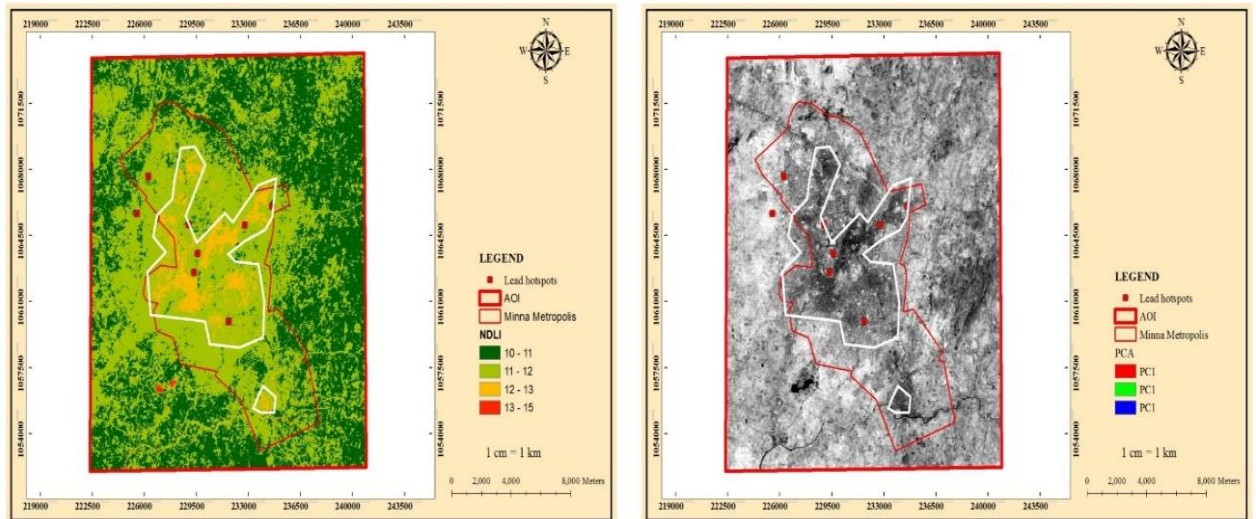
Figure 4.14: PC1 map representation

Figure 4.14 shows relatable outputs of the two geospatial techniques employed in this study for the spectral analysis of lead metal in topsoil. Since the yellow portion (indicating regions with NDLI value of 12-13) is more feasible, this is used as reference for comparing the NDLI map and PCA map of lead tailings in the soil. White polygons seen in the NDLI map is the pattern of extent of spread of lead in the top soil (for NDLI value range of 12-13). This is also seen on the PCA (PC1) map. By pattern, there is a total conformity between these two maps, hence a validation of the techniques. Location is also a basic element of image interpretation, the polygon enclosing the 12-13 NDLI value are on the same locations on the two maps. This implies that there is a positive correlation between these methods and they both map the spectral reflectance of lead metal within the study area.

4.5   Laboratory Investigation of Presence of Lead in Soil

4.5.1   Atomic absorption spectrometer result

Having collected soil samples from the hotspots location, the concentration of lead

metals in them was evaluated using AAS test and the needful result excerpt from the

laboratory is presented in table 4.6.

Table 4.6: AAS Results

Localities	POINT_X (m)	POINT_Y (m)	Lead concentration (ppm)	Intensity of lead in soil
Maitumbi	234597.2061	1065974.528	14.27	574.29
Bosso	226278.0922	1067527.667	18.85	824.28
Stadium area	229580.7447	1063439.519	-0.60	-3.39
Maitumbi GRA	232768.1253	1064956.033	-0.68	-23.43
Government Sec.	228966.6017	1064975.116	1.49	54.85
Mapi	231669.0697	1059846.334	6.15	228.19
Mechanic village	229343.2163	1062450.176	23.00	1178.50
Dutsen Kura	225503.6996	1065569.943	9.53	376.18

The fourth column of table 4.6 is the concentration of lead in each mapped lead-

polluted soil in the area of interest (measured in ppm), the last column is the intensity

(how visibly reflecting) of lead in the soil locations. The lead-polluted soil hotspot at

Mechanic village is seen to be the most polluted among the eight (8) locations, followed

by Bosso and Maitumbi. The hotspot location at Mechanic village was found to be filled

with waste metallic substances and burnt particles with silvery and shinning substances (with property close to physical properties of lead) visible to the eyes. Bosso and Maitumbi are two major localities with a lot of industrial activities and soil in these areas are expected to be more polluted with lead metal than other concerned locations (except Mechanic village) since They are the most susceptible to lead pollution from human-made processes, traffic emissions (vehicle exhaust particles, tire wear particles, weathered street surface particles, and brake lining wear particles), industrial emissions (power plants, coal combustion, metallurgical industry, auto repair shops, chemical plants, food processing plants), domestic emissions, and weathering of buildings, among other causes. Notably, Stadium area and Maitumbi GRA, detected to contain lead, are seen to have ppm value (of lead metal concentration) less than 0. This implies that these locations are free from lead metals with soil in Maitumbi GRA less prone from that of Stadium Area. This contrary result from the lab is suggesting a need for fine tuning the developed NDLI model, to ensure an optimum performance, with high level of accuracy at mapping the presence of lead in soil. Less to talk about, there is a strong and positive relationship between the intensity of lead in soil within the area of interest and their respective level of concentration of lead in these locations (measured in ppm). Full result of the AAS test is attached to this report (as Appendix A).

However, the level of lead concentrations in the soil hotspots within the area of study as evaluated from AAS test are lower than the threshold values that are regarded harmful (seen in table 3.6) according to Richard (2010) and USEPA (2010). To further investigate the reliability of the model and geospatial technique developed by this study, a statistical analysis that compare NDLI value of each hotspot, their respective intensity and level of concentration was performed.

4.5.2   Comparative analysis of geospatial and laboratory outputs

Distinct NDLI values of each of the selected lead-polluted soil hotspots were extracted from Arcmap environment, by changing the symbology from classified values to unique values, and the NDLI value from each raster position of the soils extracted. These values have been placed (table 4.7) side-by-side with the intensity and level of concentration of lead in soil of these hotspots' locations.

Table 4.7: NDLI, ppm and intensity of sampled (hotspot) soil

Localities	NDLI values	Lead concentration (ppm)	Intensity of lead in soil
Maitumbi	14.32	14.27	574.29
Bosso	14.81	18.85	824.28
Stadium area	13.09	-9.60	-330.91
Maitumbi GRA	13.02	-0.68	-23.43
Government Sec.	13.84	1.49	54.85
Mapi	14.06	6.15	228.19
Mechanic village	15.00	23.00	1178.50
Dutsen Kura	14.44	9.53	376.18

Figure 4.15 shows the graphical representation of the relationship that exists between the geospatial approach of detecting lead in soil and laboratory approach (Atomic Absorption Spectrometer test).
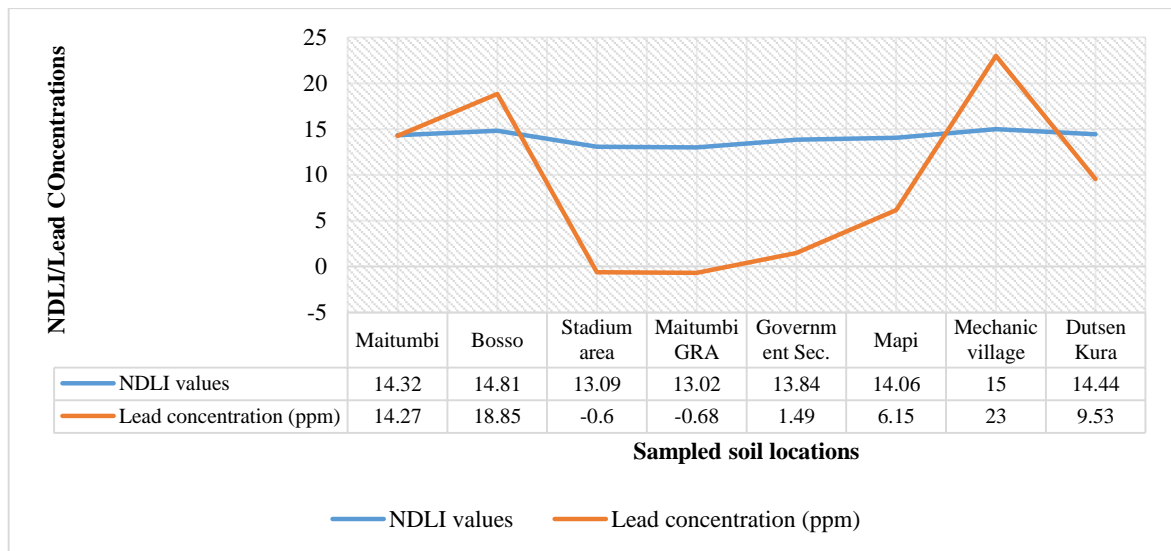
	Maitumbi	Bosso	Stadium area	Maitumbi GRA	Government Sec.	Mapi	Mechanic village	Dutsen Kura
NDLI values	14.32	14.81	13.09	13.02	13.84	14.06	15	14.44
Lead concentration (ppm)	14.27	18.85	-0.6	-0.68	1.49	6.15	23	9.53

Figure 4.15: Relationship between NDLI and level of concentration of lead in sampled

soil

Graph of NDLI values of sampled soil is seen to have a linear and zig-zag-shape; high

values from Maitumbi through Bosso then lower values through Stadium area, Maitumbi

GRA and Government Secretariat then an increase at Mechanic village (the location with

highest NDLI value) and finally a decrease again through Dutsen Kura. On the other hand,

lead concentration (in ppm) across these locations show an irregular pattern. Figure 4.16

shows the graphical representation of NDLI values, level of concentration and intensity
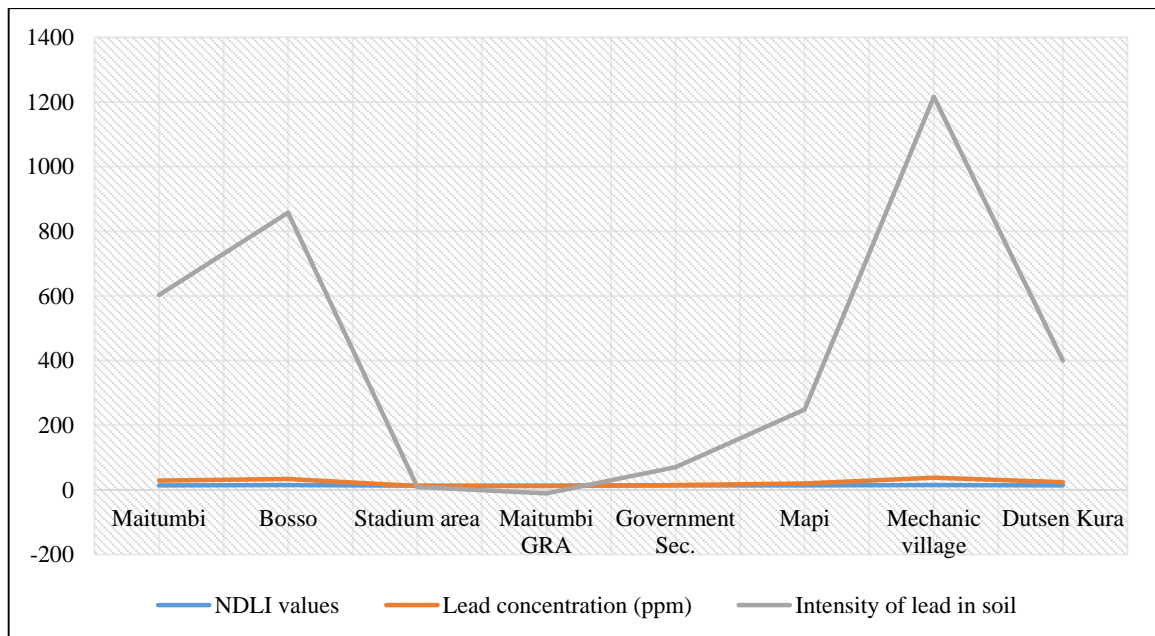
of lead in sampled soil.

Figure 4.16: Relationship between NDLI, level of concentration and intensity of lead in sampled soil

To find out the type of relationship that exists between geospatial technique (using NDLI values) and laboratory test result (from AAS), correlation and regression analysis were performed on these parameters.

4.5.3 Statistical analysis between parameters

Table 4.8 shows the output of correlation analysis performed among the parameters, consequentially, between the compared approaches. The table contains the correlation between NDLI values and levels of lead concentration, Pearson correlation between lead concentration and intensity and relationship that exists between NDLI values and intensity of lead in sampled soil. The table shows that there is a 98.9% significant correlation (at 99.9% level of confidence) between intensity of lead and corresponding level of concentration in soil. This implies that the brighter lead can be seen in soil is higher the level of its concentration in such soil.

Table 4.8: Correlation Analysis

Correlations

		NDLI_values	Pb_Conc	Pb_Intensity
NDLI_values	Pearson Correlation	1	.935[**]	.903[**]
	Sig. (2-tailed)		.001	.002
	N	8	8	8
Pb_Conc	Pearson Correlation	.935[**]	1	.989[**]
	Sig. (2-tailed)	.001		.000
	N	8	8	8
Pb_Intensity	Pearson Correlation	.903[**]	.989[**]	1
	Sig. (2-tailed)	.002	.000	
	N	8	8	8

Also, the table shows that there is a strong positive correlation (0.935) between NDLI values and level of concentration of lead in the soil. This relationship is the same that exists between NDLI values and intensity of lead in the soil. When NDLI values of samples of soil is relatively known, level of concentration of lead in the sampled soils can be judged to be directly proportional to the NDLI values, with 98% reliability.

Table 4.9 shows the output of regression analysis performed to model the relationship that exists between NDLI values and level of concentration of lead metal in top soil.

Table 4.9: Regression analysis

4.9a: Model Summary

Model	R	R Square	Adjusted R Square	Std. Error of the Estimate
1	.989[a]	.978	.975	68.90383

4.9b: ANOVA[a]

Model		Sum of Squares	df	Mean Square	F	Sig.
1	Regression	1279186.187	1	1279186.187	269.431	.000[b]
	Residual	28486.423	6	4747.737		
	Total	1307672.610	7			

a. Dependent Variable: Pb_Intensity

b. Predictors: (Constant), Pb_Conc

4.9c: Coefficients[a]

Model		Unstandardized Coefficients		Standardized Coefficients		
		B	Std. Error	Beta	t	Sig.
1	(Constant)	-24.686	35.589		-.694	.514
	Pb_Conc	47.312	2.882	.989	16.414	.000

a. Dependent Variable: Pb_Intensity

CHAPTER FIVE

5.0   CONCLUSION AND RECOMMENDATIONS

5.1   Summary

This research study was motivated by the need to explore geospatial tool, a sophisticated, fast and near-real-time monitoring technique, for detecting and monitoring lead tailings in soil. Having explored Snell's law and law of refraction in physics, integrated with understanding of the electromagnetic spectrum, an index (NDLI) capable of detecting presence of lead was developed in this study. This index was used to investigate the presence of lead and extent of its spread across and beyond Minna Metropolis (an area of interest); this however was done using Landsat 8 OLI imageries (two different dataset) acquired in April and June, 2021, June being the start of this study. This was needful to verify the developed model and to avoid any error due to geometric displacement of Landsat imageries. PCA was also used to minimize the number of data, by exploring which of the spectral bands of Landsat 8 OLI is enough for mapping lead spread in top soil. Lead-polluted soil hotspots were pointed out from NDLI map using soil locations with highest range of NDLI values. These locations were 'ground-truthed' and samples of these polluted soils were taken to the laboratory for Atomic Absorption Spectrometry test (a laboratory test required for detecting the presence, intensity and concentration of lead metal in soil).

In order to estimate the accuracy of NDLI values by comparing with laboratory result, graphical and statistical analyses were performed using NDLI values (from geospatial technique), level of concentration and intensity of lead in sampled soil (from AAS test). Correlation analysis was performed to estimate the degree of closeness of output from geospatial technique and laboratory, relationship that exists between these techniques.

Also, regression analysis was also performed on these parameters in order to model the type of relationship that exists between the two techniques under study.

5.2   Conclusion

The aim of this study is to explore the applicability of geospatial tools for detecting lead pollution in top soil. Normalized Difference Lead Index developed in this study was found capable of detecting lead in top soil. Outputs from implementation of this index over two but different time-series Landsat 8 OLI imageries were found agreeing, also, PCA analysis carried out has its output synonymous to that of the NDLI maps. From comparison carried out using eight detected lead hotspots and soil samples taken from these locations, according to the laboratory result (considered as de-facto in this research), two out of these locations (Maitumbi GRA and Stadium Area) were found free from lead metal pollution (with level of concentration of lead in these locations yielding negative), contrary to their NDLI values which implied presence of lead higher than many other parts of the study area. However, other sampled soils were found polluted with lead in synchrony with their respective NDLI values. From statistical analysis performed, there is a 70% positive correlation between geospatial technique and AAS test and this relationship has been modeled from regression analysis.

It is worth noting that the level of concentration of lead metal in the sampled soil (mapped as most polluted in the area of interest) is found below the scientifically established threshold known to be very harmful to human health. Conclusively, geospatial technique, using the developed index in this study can give an approximate result to the detection of lead in top soil and can be used to monitor the spread of such harmful metal, an improvement over the weakness of laboratory approach.

5.3   Recommendations

1. Sampled soil from Maitumbi GRA and Stadium Area should be investigated for possibility of presence of other heavy metal, with physical property(ies) close to that of lead (Pb) since the implemented index mapped soil within these locations as lead-polluted

2. Effect of seasonal changes or variations on the performance of the developed index should be studied

3. Periodic monitoring of lead concentration and its spread should be considered over the area of study

4. Water bodies around Mechanic village should be tested, and if channeled to Minna Water board, lead-metal remediation chemicals or treatment should be considered

5. Children should be controlled around hotspot locations, since they are the most vulnerable to lead pollution in this area, due to intake of soil

REFERENCES

Latif, F., Wani A. A and Usmani. J, A (2015). Lead Toxicity: A review. Interdisciplinary Toxicity (8), (55).pp 234-245

Abdel-Sabour, M. F.; Abdou, F. M.; Elwan, I. M.; Al-Salama, Y. J. 2002. Effect of soil contamination due to wastewater irrigation on Cr fractions in some soils of Egypt. Proc. 6th Radiation Physics Conf., Assuit, Egypt. 27-30.

Abdullahi, M. S. (2013). Toxic effects of lead in humans: an overview. *Global Advanced Research Journal of Environmental Science and Toxicology (GARJEST),* 2(6), 157-162

Abidemi, O. O. (2011). Levels of Pb, Fe, Cd and Co in Soils of Automobile Workshop in Osun State, Nigeria. Journal of Applied Sciences and Environmental Management volume 15, issue no. 2. Doi: https://www.doi.org/10.4314/jasem.v15i2.68510

Abu Khatita, A. M. 2011. Assessment of soil and sediment contamination in the Middle Nile Delta area (Egypt)- Geo-Environmental study using combined sedimentological, geophysical and geochemical methods. German, Alexander-Universität ErlangenNürnberg zur Erlangung.

Acton, Q. A., ed. (2013). Issues in Global Environment—Pollution and Waste Management: 2012 Edition. ScholarlyEditions. ISBN 978-1-4816-4665-9.

Adriano, D. C. (2001). Trace elements in terrestrial environments; biochemistry, bioavailability and risks of metals. Springe, New York.

Alloway B.J (1995). Heavy metals in soils. Blackie Academics and professional, chapman and Hall London, 368P. https://doi.org/10.1007/ 9.78-94 011-1344-1.

Aloysius, A. P., Rufus, S. & John, O. O. (2013). Evaluation of heavy metals in soils around auto mechanic workshop clusters in Gboko and Makurdi, Central Nigeria. *Journal of Environmental Chemistry and Ecotoxicoloy,* 5(11), 298-306.

Alsfasser, R. (2007). Moderne anorganische Chemie [Modern inorganic chemistry] (in German). Walter de Gruyter. ISBN 978-3-11-019060-1.

Angelika, E. C. & Jeffrey, R. B. (2020). Lead Toxicity and Pollution in Poland. *International Journal of Environmental Research and Public Health,* 17(4385), 1-14

Aronsson, P. & Perttu K. (2001). Willow vegetation filters for wastewater treatment and soil remediation combined with biomass production. For. Chron., 77, 293-299

ATSDR. (2019). Lead Toxicity: Case Studies in Environmental Medicine (CSEM). Environmental Health and Medicine

ATSDR.(2017). Lead Toxicity: What is the biological Fate of Lead in the Body? Environmental Health and Medicine Education. 2017. Available online: https://www.atsdr.cdc.gov/csem/csem.asp?csem=34&po=9 (accessed on 12 June 2017).

Avery, U and Berlin, L (1992). (Fundamentals of Remote sensing and airphotos interpretation (pp 472) upper saddle river, NJ prentice Hall, New York.

Baird, C and Cann, N. (2012). Environmental Chemistry (5th ed.). W. H. Freeman and Company. ISBN 978-1-4292-7704-4

Bernado, J. F. (2020). Aluminium Toxicity. Available online: https://emedicine.medscape.com/article/165315-overview#showall, accessed on October 19, 2020.

Beyersmann, D. & Hartwig, A. (2008). Carcinogenic metal compounds: recent insight into molecular and cellular mechanisms. *Arch Toxicol,* 82(8), 493-512

Bharara, M. S and Atwood, D. A. (2006). *″*Lead: Inorganic ChemistryBased in part on the article Lead: Inorganic Chemistry by Philip G. Harrison which appeared in theEncyclopedia of Inorganic Chemistry, First Edition". Lead: Inorganic Chemistry. doi*:*10.1002/0470862106.ia118. ISBN 978-0470860786.

Chang LW, Magos L, Suzuki T (eds.) (1996) *Toxicology of Metals.* CRC Press, Boca Raton. FL, USA

Daniel, Ž, Anna, J., Tereza, Z, Kateřina, Z and Robert, M (2019). Mapping soil degradation using remote sensing data and ancilliary data: South-East Moravia,

Czech Republic. European Journal of Remote Sensing, Volume 52, issue no. 1, pp. 108-122.

Doctors without Borders (2010):- Lead poisoning crisis in Zamfara state northern Nigeria; Http;//www.doctors without border.dr accessed date 23/3/2021.

Duffus J. H (2002). Heavy metals, a meaningless term? Pure and Applied Chemistry, volume 74, pp. 793-807

Duruibe J. O, Ogwuegbu M. O., Egwurugwu J. N (2014). Heavy metal pollution and human biotoxic effects. International Journal of physical sciences, volume 2, issu no. 5, pp. 112-118.

Ede, A and Cormack, L. B. (2016). A History of Science in Society, Volume I: From the Ancient Greeks to the Scientific Revolution, Third Edition. University of Toronto Press. ISBN 978-1-4426-3503-6

Fergusson, J. E (eds.) (1990). The Heavy Elements: Chemistry, Environmental Impact and Health Effects. Pergamon Press. Oxford

Freeman, K. S. (2012). "Remediating soil lead with fishbones". Environmental Health Perspectives. *120 (1): a20–a21.* doi:10.1289/ehp.120-a20a. PMC 3261960. PMID 22214821

Fu, F and Wang, Q. (2011). Removal of heavy metal ions from wastewaters: A review. Journal of Environmental Management, volume 92, issue no. 3, pp. 407-418.

Gautam P. K., Gautam, R.K., Chattopadhyaya, M.C. Banerjee, M.C. Chattopadhyaya, J.D. Pandey, N (2016). Heavy metals in the environment: fate, transport, toxicity and remediation technologies.

Gupta N., Khan D. K. and Santra S. C (2012). Heavy metal accumulation in vegetables grown in a long-term wastewater-irrigated agricultural land of tropical India. Journal of Environmental Monitoring and Assessment, article 184, pp. 6673-6682

Harbison, R. D., Bourgeois, M. M and Johnson, G. T. (2015). Hamilton and Hardy's Industrial Toxicology. John Wiley & Sons. ISBN 978-0-470-92973-5

Haynes, W.M. (2011). CRC Handbook of Chemistry and Physics, 92nd ed., CRC Press, Florida, 2011.

He, J. Y and Jia, X, (2004). Arc GIS geostatistical analyst application in assessment of MTBE contamination, ESRI User Conference Fremont,CA. Available at: http://gis.esri.com/library/userconf/proc04/docs/pap1628

He, Z. L, Yang, X. E, Stoffella, P. J (2005) Trace elements in agroecosystems and impacts on the environment. *Journal of Trace Elements and Medical Biology, volume 19, issues number 2-3, pp. 125-140.*

Henke, J. M and Petropoulos, G. P (2013). A GIS-based exploration of the relationships between human health, social deprivation and ecosystem services: The case of Wales, UK. Journal of Applied Geography, 45, pp. 77-88.

Herawati W, Suzuki S, Hayashi K, Rivai I.F and Koyoma H. (2000):cadium copper and zinc levels in rice and soil of Japan , Indonasia and China by soil type. Bulletin of environmental contamination and toxicity 64,pp 33-39.

Ifeoluwa, A (2018). How to end lead poisoning in Nigeria June 27,2018 www.premiumtimesng.com accessed date 16/2/2021.

Jarup, L. (2013). Hazards of Heavy metal contamination. Br Med Bull., vol. 68 (1), pp. 167-182

Jessica, B, Emmanuel, S and Renald, B (2020). Heavy metal pollution in the environment and their toxicological effects on human. Helion, volume 6, issue 9. Doi: heliyon.2020.e04691

Kabata-Pendia, A (eds.) (2001) *Trace Elements in Soils and Plants. 3rd ed.* CRC Press, Boca Raton, FL

Khilifi, R and Hamza-Chaffai, A. (2010). Head and neck cancer due to heavy metal exposure via tobacco smoking and professional exposure: A review. Journal Toxicology Application and Pharmacology, volu. 248, pp. 71-88.

Kosnett, M. J. (2006). "Lead". In Olson, K. R. (ed.). Poisoning and Drug Overdose (5th ed.). McGraw-Hill Professional. p. 238. ISBN 978-0-07-144333-3.

Lagerkvist J-S. B.; Oskarsson, A. 2007. Vanadium in Nordberg, G., Fowler, B., Nordberg, M. and Friberg, L., (Eds), Handbook on the Toxicology of Metals, Third ed. San Diego: Academic Press

Langmuir, C. H and Broecker, W. S. (2012). How to Build a Habitable Planet: The Story of Earth from the Big Bang to Humankind. Princeton University Press. ISBN 978-0-691-14006-3

Lenntech B. V (2018). Heavy metals. An online resources: www.lenntech.com/processes/heavy/heavy-metals/heavy-metals.htm, accessed on 30th October, 2020

Lillesand, T. M.; Kiefer, R. W. 2003. Remote Sensing and Image Interpretation. 2nd ed. New York:

Luo, X., Yu S., Zhu, Y.G, Li X. D (2012). Trace metal contamination in urban soils of China. Sci. Total Environ., 421, pp. 17-30.

Ming-Ho, Y. (2005). *Environmental Toxicology: Biological and Health Effects of Pollutants*, Chap. 12, CRC Press LLC, ISBN 1-56670-670-2, 2nd Edition, BocaRaton, USA.

Monisha, J, Tenzin, T, Naresh, A, Blessy, M. B. and Krishnamurthy N. B (2014). Toxicity, mechanism and health effects of some heavy metals. Journal of Interdisciplinary Toxicology, vol. 7, issue no. 2, pp. 60-72.

Muchuweti M., Brikett J. W., Chinyanga E., Zvauya R., Scrimshaw M. D and Lester J. N (2016). Heavy metal content of vegetables irrigated with mixtures of wastewater and sewage sludge in Zimbabwe: implications for human health. Journal of Agricultural Ecosystem and Environment, volume 112, pp. 41-48.

National population commission (2006):- Nigeria population census report. National population commission Abuja 21-27.

Nriagu, J. O (1989). A global assessment of natural sources of atmospheric trace metals. *Nature* 338: 47-49

Nriagu, J. O and Kim, M-J. (2000). "Emissions of lead and zinc from candles with metal-core wicks". *Science of the Total Environment*. **250** (1–3): 37–41. Bibcode:2000ScTEn.250...37N. doi:10.1016/S0048-9697(00)00359-4. PMID 10811249

Oehlenschläger, J. (2002). Identifying heavy metals in fish In: *Safety and Quality issues in fish processing*, Bremner, H.A. (Ed), pp. 95-113, Woodhead Publishing Limited, 978-1- 84569-019-9, Cambridge.

Rao C. Reddi G. S (2000). Platinum group metals (PGM); occurrence, use and recent trends in their determination. TrAC Trends in Analytical Chemistry, volume 19, issue no. 9, pp- 565-586.

Ravindra Singh and Narendra Kumar Ahinwar (2018). Review on sources and effect of heavy metal in soil: its bioremediation. International Journal of Research in applied, Natural and Social Sciences. Special edition, ISSn (P): 2347-4580, pp. 1-22

Salim, L, Paul B, and George P (2019) :- Investigating the potential of hyperspectral imaging for the quantitative estimation of lead contamination in soil. Journal of sensors MDPI (3),(2),pp 29-42.

Seema Tiwari, Tripathi I. P and Tiwaril H. L (2013). Effects of Lead on Environment. International Journal of Emerging Research in Management and Technology, volume 2, Issue 6, pp. 1-5

Simba, T., Casey, B., Ian von, L., Margrit, V., Douglas, L., Shehu, M. A and Aishat, A (2018). Food contamination as a pathway for lead exposure in children during the 2010-2013 lead poisoning epidemic in Zamfara Nigeria. Journal of Environmental Sciences, volume 67, pp. 260-272

Sinha, S. P., Shelly, V., Sharma, V. (1993). "Neurotoxic effects of lead exposure among printing press workers*". Bulletin of Environmental Contamination and Toxicology. *51 (4): 490–93.* doi*:10.1007/BF00192162.* PMID 8400649. S2CID 26631583.

Sunderman, F. W. (Jr.); Oskarsson, A. 1991. Nickel. In: Merian E (ed.) Metals and their Compounds in the Environment; Occurrence, Analysis and Biological relevance. Weinteim, Basel: VCH.

Tamayo Ortiz, M. (2016); Téllez-Rojo, M.M.; Hu, H.; Hernandez-Avila, M.; Wright, R.; Amarasiriwardena, C.;

Tchonwou P. B (2012). Heavy metals toxicity and the environment. EXS., 133-164.

Terfassa, B, Schachner, J. A., Traar, P., Belaj, F. & Zanetti, N. C. (2014). Oxorhenium(V) complexes with naphtholate-oxazoline ligands in the catalytic epoxidation of olefins. Polyhedron.

USEPA (2010). Land Application of bio solids for home vegetable gardens. USEPA clean water act title 40, section 503.13.

Walker, C. H., Sibly, S. P. & Hopkin, D. B. (2012). Principles of Ecotoxicology; Group T. and F., 4th edition, CRC Press.

WHO (2016). Expert Consultation. Available evidence for the future update of the WHO Global Air Quality Guidelines (AQGs). Available online: https://www.euro.who.int/_data/assets/pdf_file/0013/301720/evidence-future-update-AQGs-mtg-report-Bonn-sept-oct-a5.pdf (Accessed on 3rd November, 2020)

WHO (2019). 'Exposure to Lead: A Major Public Health Concern' accessed at: https://apps.who.int/iris/bitstream/handle/10665/329953/WHO-CED-PHE-EPE-19.4.7-eng.pdf?ua=1

World Health Organization (WHO) (1996). *Trace Elements in Human Nutrition and Health*. World Health Organization. Geneva, Switzerland.

Wieczorek, J., Baran, A., Urbanski, K., Mazurek, R. & Klimowicz-Pawals, A. (2020). Assessment of the pollution and ecological risk of lead and cadmium in soils. Journal of Environment and Geochemical Health. 40, 2325-2342.

Woo, K. S.; Jo, J. H.; Basu, P. K.; Ahn, J. S. 2009. Stress intensity factor by p-adaptive refinement based on ordinary Kriging interpolation, Finite Elem. Anal. Des. 45(3):227-234.

Yuan, F., Linlin, X., Junhuan, Pen1, H., Wang, A. W. & David, A. C. (2018). Retrieval and Mapping of heavy metal concentration in soil using time series Landsat 8 Imagery. The International Archives of the Photogrammetry, Remote Sensing and Spatial Information Sciences, XLII-3, 335-340.

Yusuf, M., Elfghi, F.M., Zaidi, S.A., Abdullah, E.C. & Khan, M. A. (2015). Applications of graphene and its derivatives as an adsorbent for heavy metal and dye removal: A systematic and comprehensive overview. RSC Advances. 5, 50392-50420

Zheng, C. 2006. Using multivariate analyses and GIS to identify pollutants and their spatial patterns in urban soils in Galway, Ireland. Environmental Pollution. 142(3):501-511.